



Nano Electro Mechanical Systems (NEMS) and interactions at nanoscale

Alessandro Siria:

Institut Néel-CNRS Grenoble
CEA-LETI/MINATEC Grenoble

Advisors:

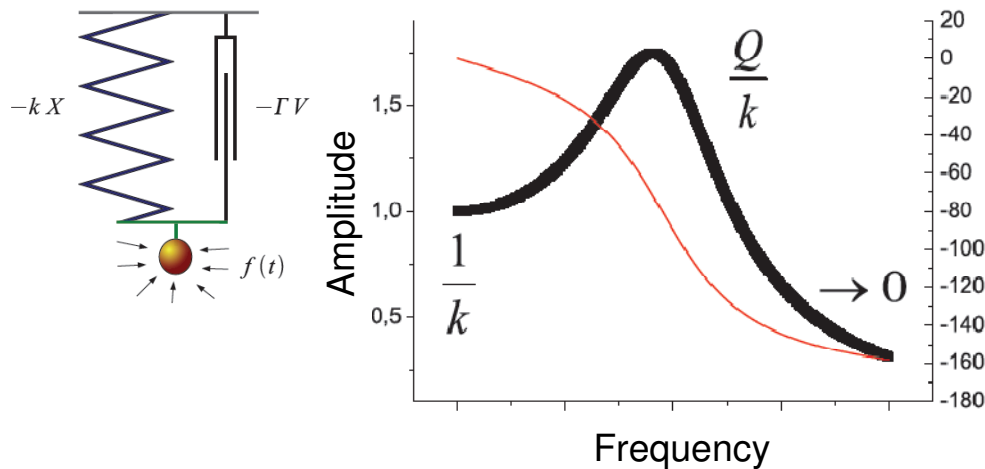
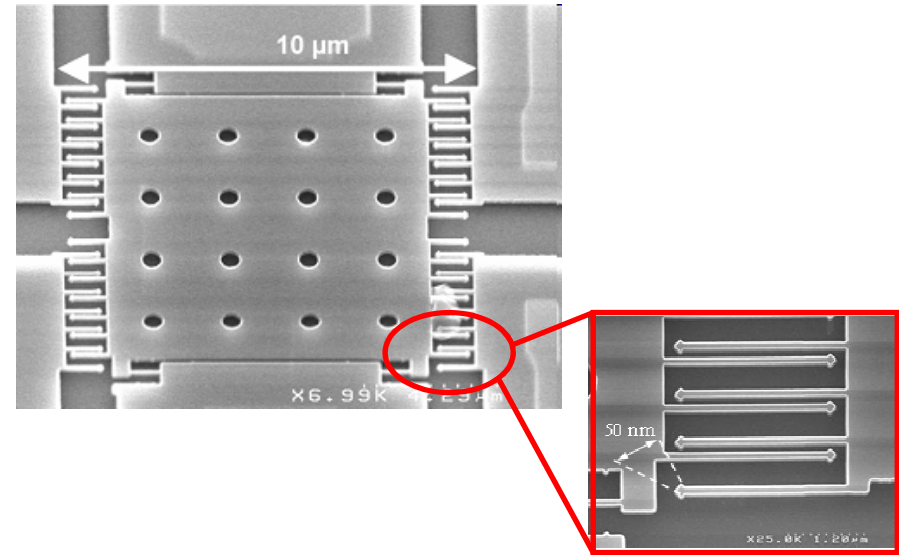
Joel Chevrier, UJF and CNRS Grenoble

Hubert Grange, CEA-LETI/MINATEC Grenoble



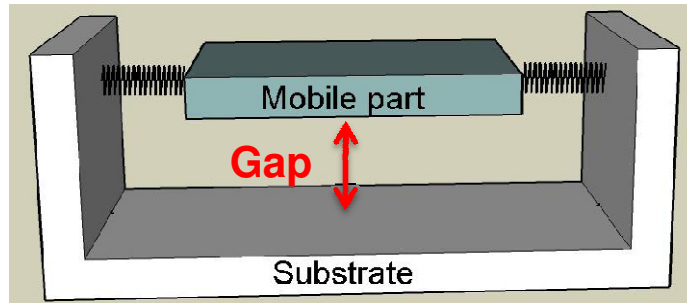
NEMS are devices integrating electrical and mechanical functionalities at the nanoscale.

NEMS are among the best candidates for measurement of interactions at nanoscale



NEMS resonators can be assimilated to harmonic oscillators

$$\chi(\omega) = \frac{1}{m(\omega_0^2 - \omega^2) + i\gamma\omega}$$



NEMS standard scheme:

- Mobile part suspended over a fixed substrate;
- Gap from tens nanometers to several microns;
- Plane-Plane geometry.

Interactions between mobile and fixed parts can dominate the NEMS dynamics

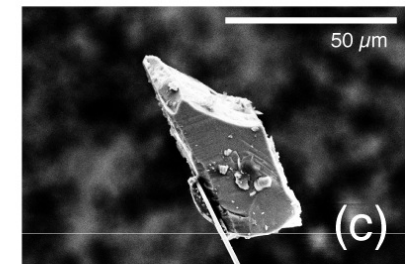
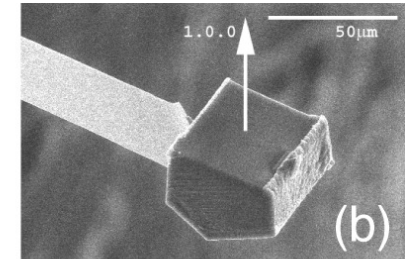
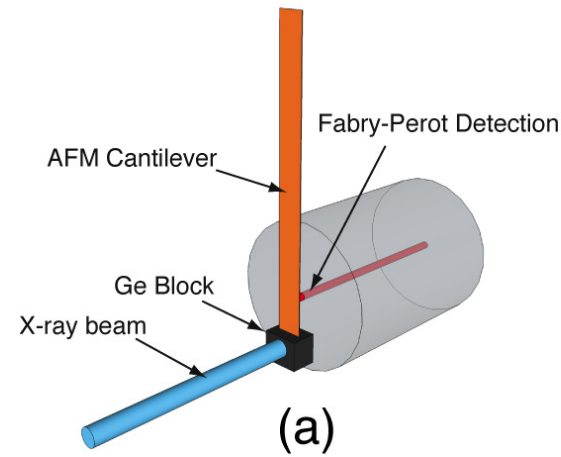
- Chemical forces;
- Van der Waals and Casimir forces
- Electrostatic (residual) forces;
- Optical forces;
- Hydrodynamic forces;
- Near field thermal radiation.

- Detection set-up: fibre-based optical interferometry.
- Hydrodynamic forces at micron and submicron scale:
 1. Cavity damping of a microlever;
 2. Cavity freezing of a microlever.
- Radiative heat transfer at nanoscale:
 1. Electromagnetic treatment of thermal radiation;
 2. Radiative heat transfer between a sphere and a plane.
- Conclusions and perspectives.

OPTICAL FORCES

Interaction between X-ray and Mechanical systems:

- 1) Mechanical effect of X-ray beam;
- 2) MEMS based X-ray chopper.

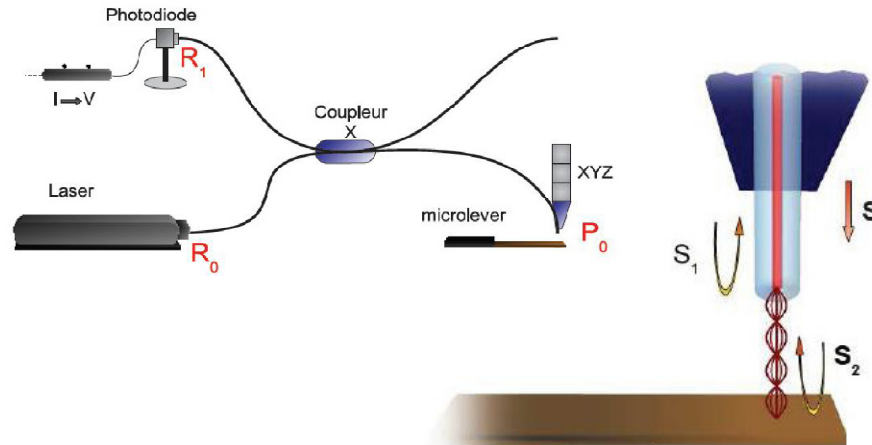


European Synchrotron Radiation Facility

@ Surface Science Laboratory (SSL)

In collaboration with
Fabio Comin

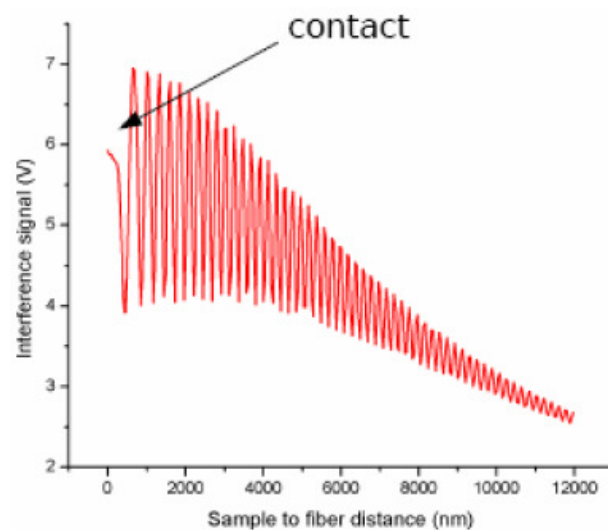
Detection set-up: optical interferometry



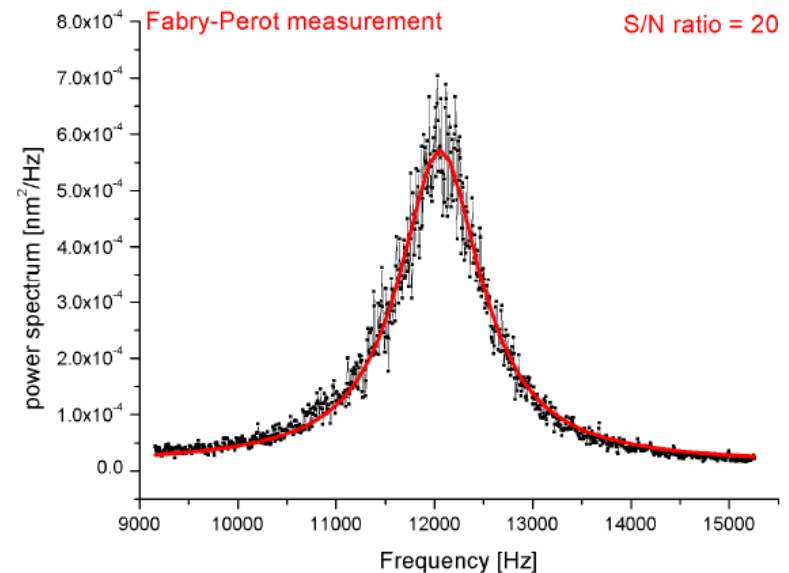
Fabry Perot cavity formed between the fibre end and the sample surface

Movement of the surface is translated in detectable light intensity modulation.

$$I_{ph}(d) = I_1 + I_2 + 2\sqrt{I_1 I_2} \sin\left(\frac{4\pi}{\lambda} d + \varphi\right)$$



$$Sensibility < 10^{-12} \text{ m}/\sqrt{\text{Hz}}$$

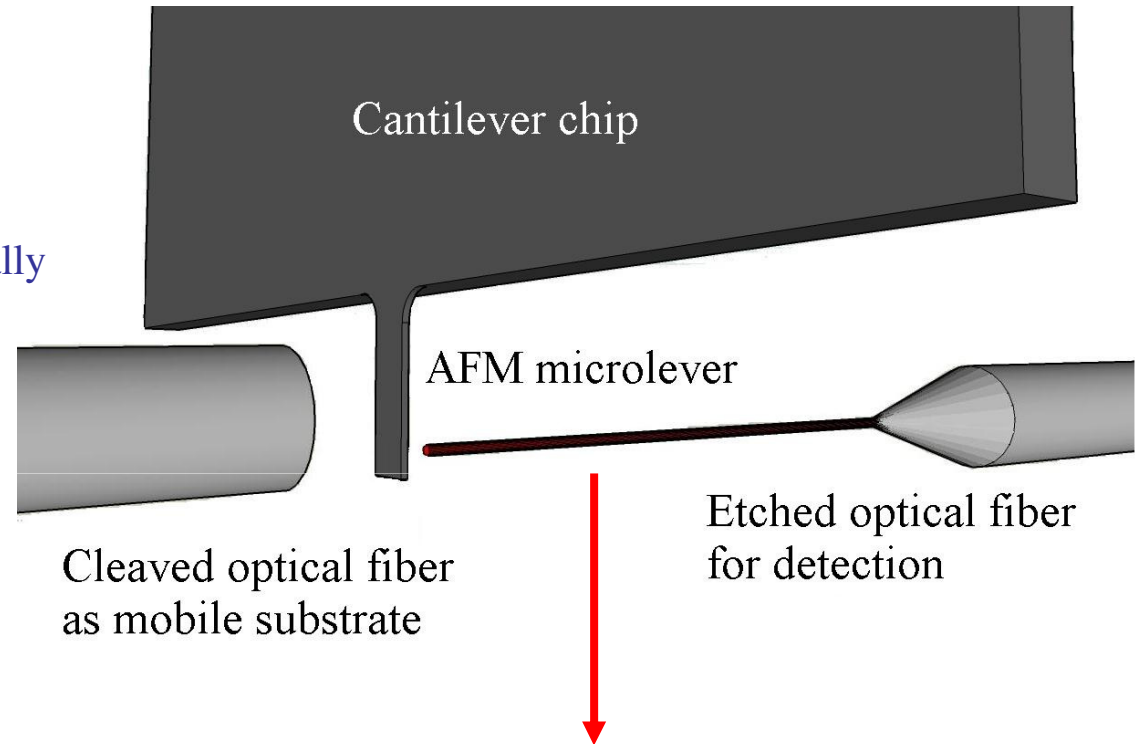


Microlever Brownian motion detection

Hydrodynamic forces at micron and sub-micron scale

Hydrodynamic forces at short distances

The oscillating behavior of a lever is studied when an “infinite” wall is gradually approached.



This system mimics a MEMS oscillating closed to a substrate

Si cantilever:

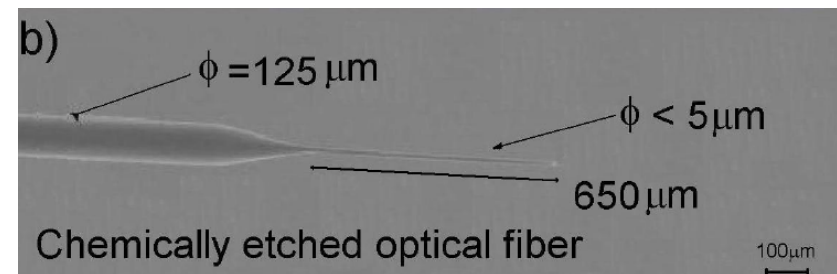
$L = 107 \mu\text{m}$

$w = 30 \mu\text{m}$

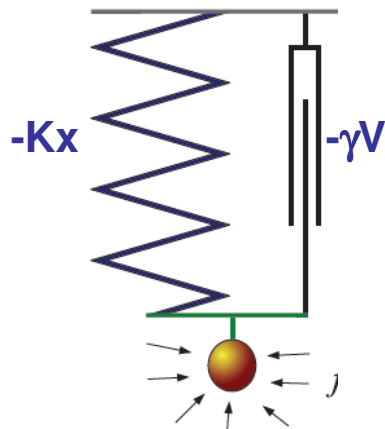
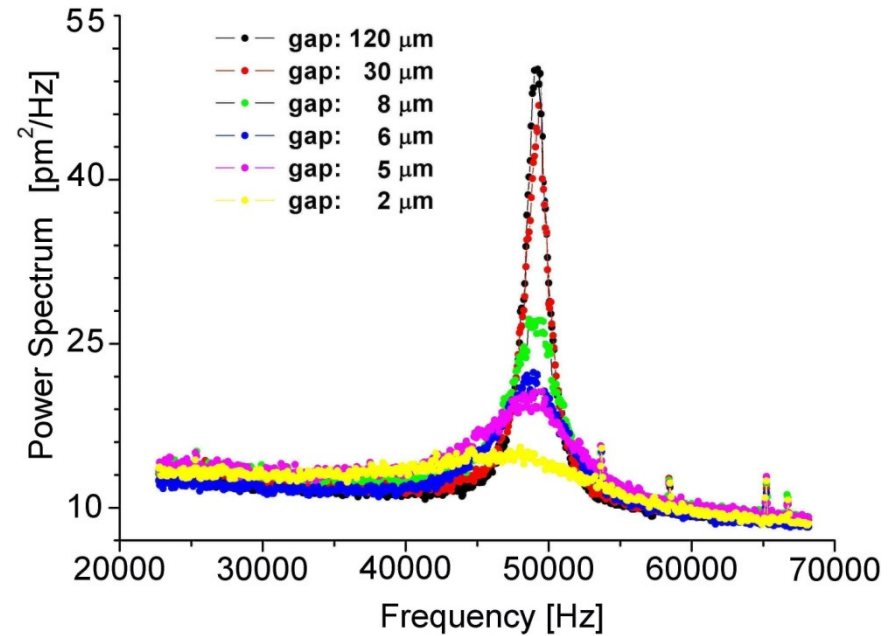
$t = 0.18 \mu\text{m}$

$\omega_0/2\pi \approx 50 \text{ kHz}$

No additional damping



The lever is thermally actuated.
 With decreasing gap in micrometer range we observe a broadening and softening of fundamental resonance.



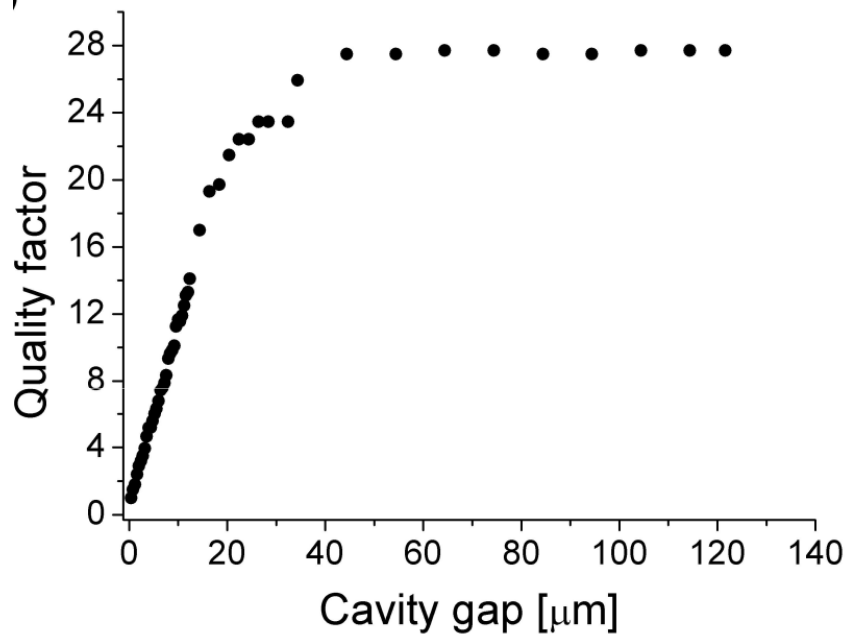
Driven and damped 1D oscillator

$$\chi(\omega) = \frac{1}{m(\omega_0^2 - \omega^2) + i\gamma\omega}$$

Damping of lever studied recording resonance quality factor

$$Q = \frac{\Delta\omega}{\omega_{res}} = \frac{k}{\omega_0\gamma}$$

Broadening:

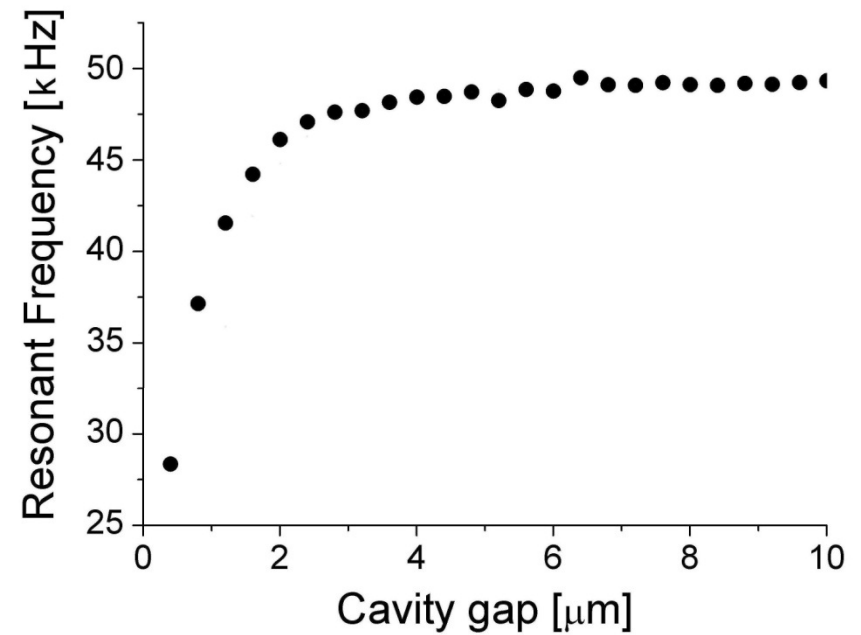


Micrometric length scale:

$$d_L \approx 20 \mu\text{m}$$

Confinement effect

Softening:

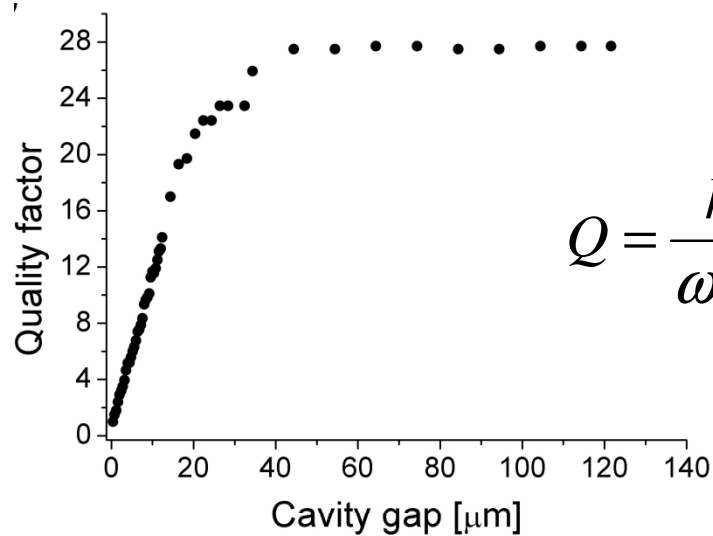


Nanometric length scale:

$$d_C \approx 400 \text{nm}$$

Freezing of resonance

Cavity damping of the oscillator



$$Q = \frac{k}{\omega_0 \gamma}$$

Large gap: damping independent on distance

Small gap : damping depending on inverse of distance

Theoretical description based on Navier-Stokes equation

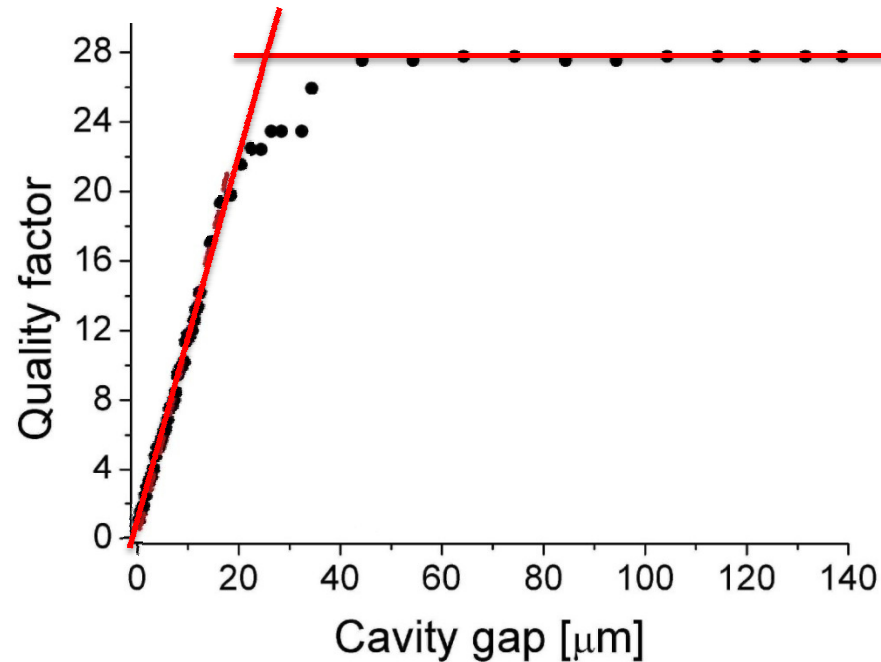
$$\rho \left[\frac{\partial \vec{v}}{\partial t} \right] = \eta \nabla^2 \vec{v} - \nabla p$$

Reynold's number: $Re = \frac{v \cdot d \cdot \rho}{\eta} \approx 10^{-6} \div 10^{-4}$ **LAMINAR REGIME**

Which boundary conditions??

Boundary conditions control the agreement theory - experiments

Confinement characteristic length



Boundary layer definition: $d_L = \sqrt{\frac{2\eta}{\rho\omega}}$

At lever resonance: $d_L \approx 20\mu m$

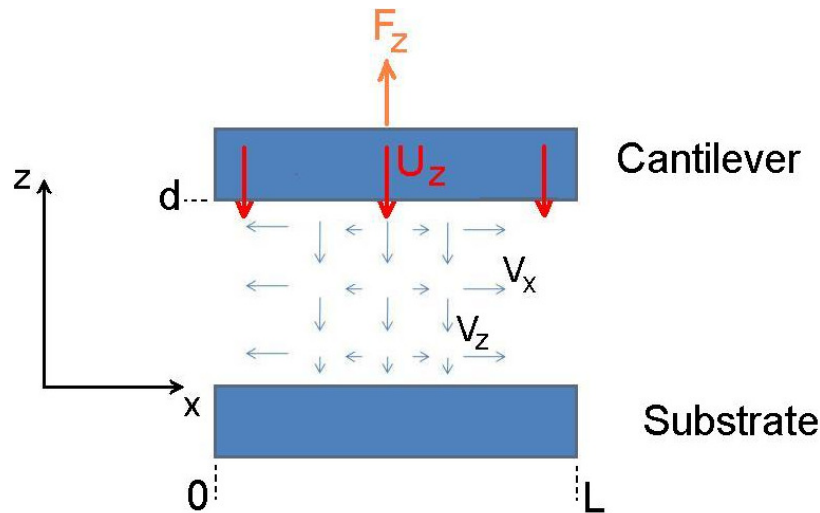
Spatial region surrounding the lever where viscosity dominates the fluid behavior

$$\frac{\rho \left[\frac{\partial \vec{v}}{\partial t} \right]}{\eta \nabla^2 \vec{v}} \approx \frac{\rho \omega d^2}{\eta} \approx \frac{d^2}{d_L^2}$$

$d \ll d_L \Rightarrow$ Inertial \ll Viscosity

$$\eta \nabla^2 \vec{v} = \nabla p$$

Perfect slip boundary conditions



$$v_z = g(z)$$

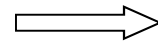
$$v_x = f(x)$$

Perfect slip at fluid-solid interface:

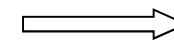
Navier-Stokes equation

$$\frac{\partial p}{\partial x} = \eta \frac{\partial^2 v_x}{\partial x^2}$$

$$\frac{\partial p}{\partial z} = \eta \frac{\partial^2 v_z}{\partial z^2}$$



$$F_z = -\frac{2\eta A}{d} U_z$$

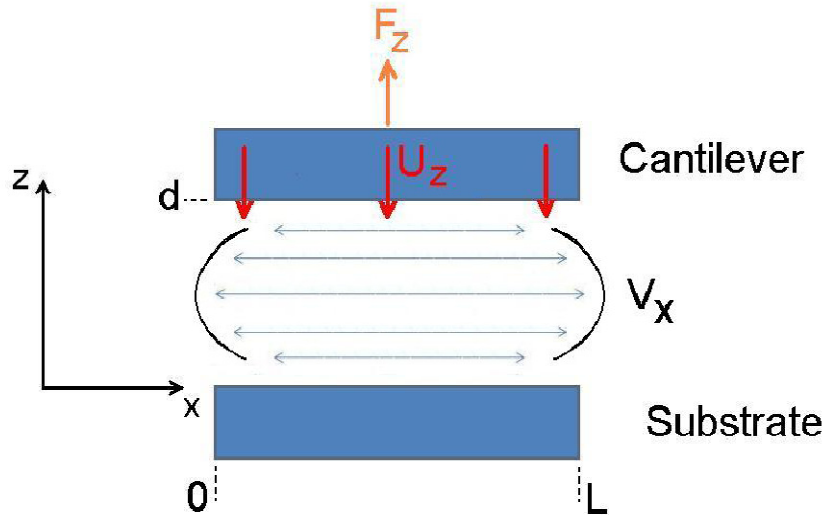


$$\gamma = \frac{2\eta A}{d}$$

$$Q = \frac{k}{2\eta A \omega_0} d$$

Linear dependency of the quality factor with the gap size.
Consistent with experimental evidence

No slip boundary conditions (Couette)



No slip at fluid-solid interface:

$$v_x(z=0) = 0$$

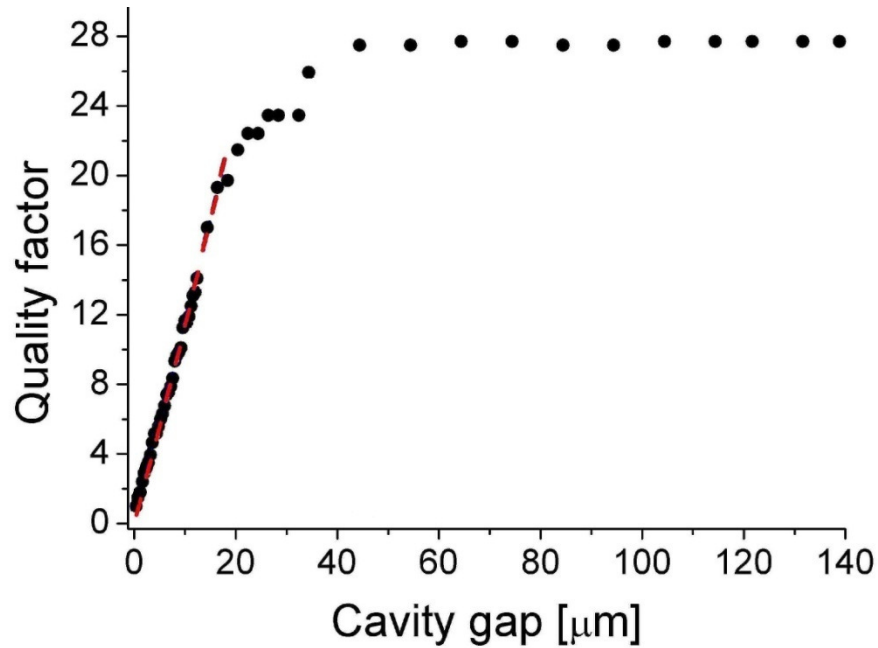
$$v_x(z=d) = 0$$

Navier-Stokes equation $\frac{\partial p}{\partial x} = \eta \frac{\partial^2 v_x}{\partial z^2} \implies F_z = -\frac{\eta L^3 w}{d^3} U_z \implies \gamma = \frac{\eta L^3 w}{d^3}$

$$Q = \frac{k}{\eta L^3 w \omega_0} d^3$$

NOT Consistent with experiments

Comparison Experiments-Theory



- Experimental data
- Theoretical model (perfect slip)

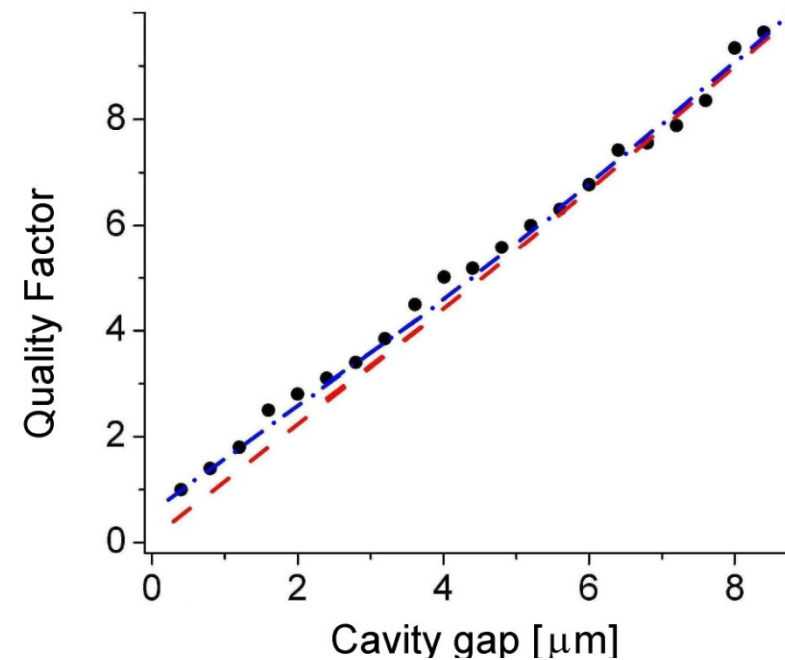
$$Q = \frac{k}{2\eta A \omega_0} d$$

No adjustable parameter

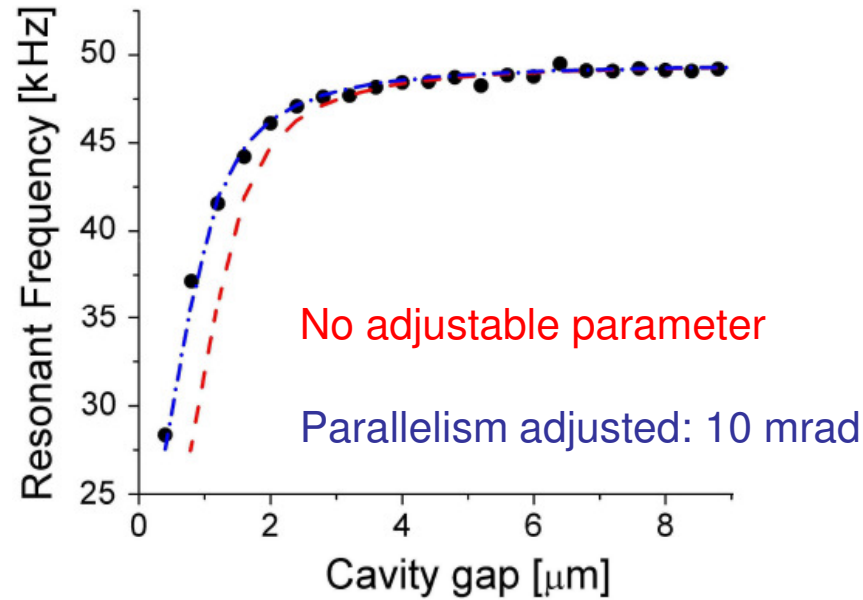
No adjustable parameter: 80% error at 400 nm

Parallelism adjusted: 5% error at 400 nm

Residual misalignment : 10 mrad



Cavity freezing of the oscillator

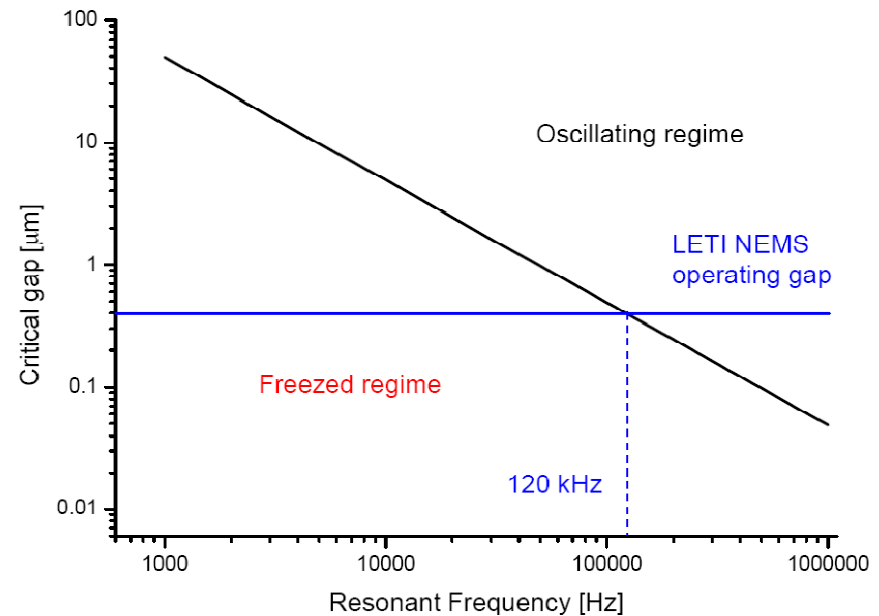


In the limit of large damping the oscillator has a down-shift of the resonance

$$\omega' = \sqrt{\omega_0^2 - \frac{1}{2} \left(\frac{\gamma}{m}\right)^2}$$

If the gap is small enough air confinement can eventually freeze the mechanical oscillator

$$Gap_{crit} = \frac{\sqrt{2}\eta}{m} \frac{A}{\omega_0} \Leftrightarrow \omega' = 0$$

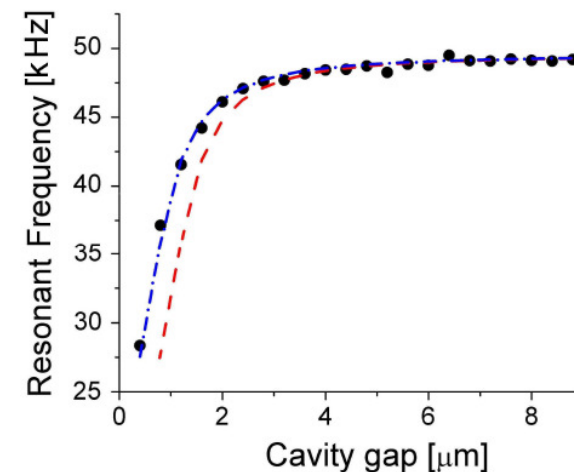
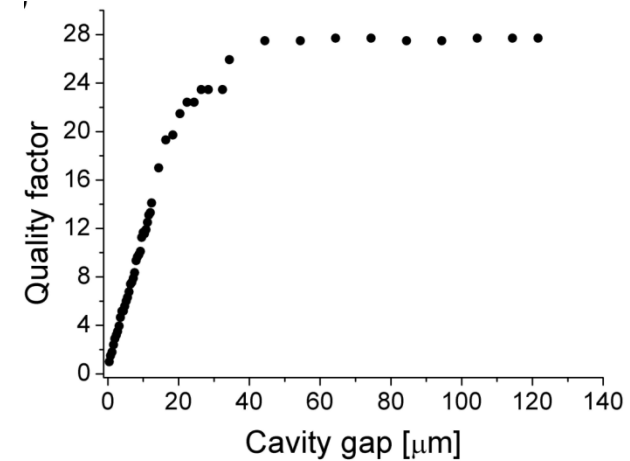


Hydrodynamic forces: summary

Cantilever dynamics modified by fluid confinement according to Navier-Stokes equation;

Perfect slip at fluid-solid interface induces a long range hydrodynamic force: $F \rightarrow 1/d$

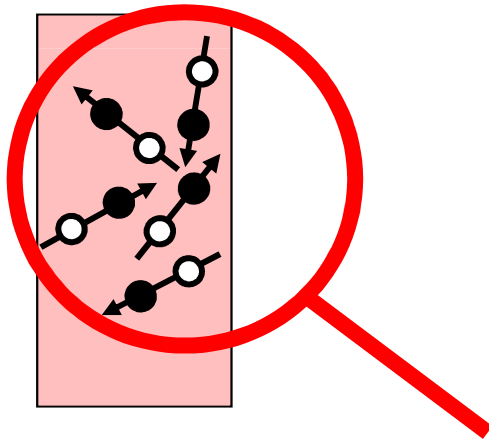
For nanometre size cavity the lever oscillation can be freezed because of the fluid confinement.



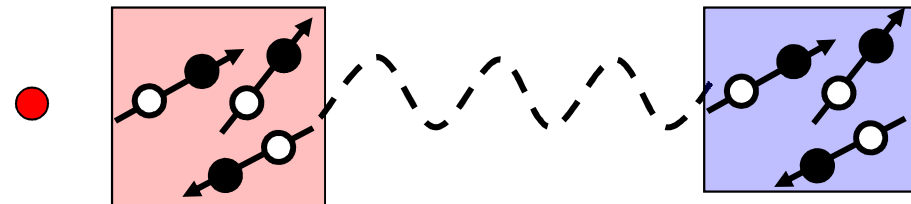
Near – Field radiative heat transfer

Electromagnetic treatment.

Fluctuating dipole
induced by thermal effect

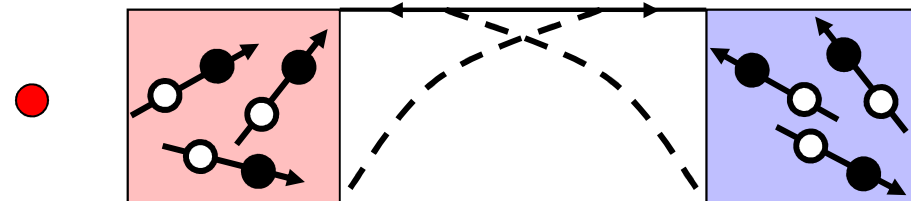


FAR-FIELD: propagative waves



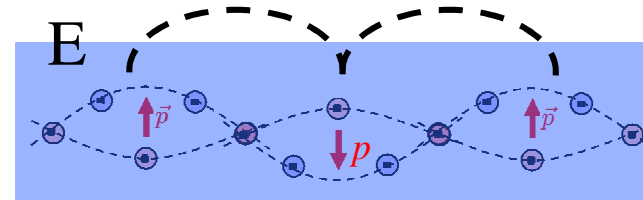
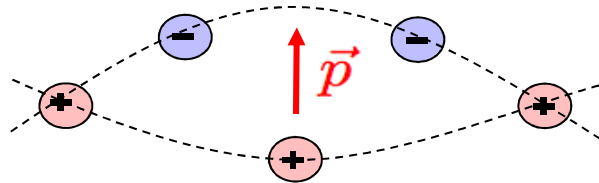
Independent by distance

NEAR-FIELD: evanescent waves



Strongly dependent by distance

Dielectric materials: surface Phonon-Polariton enhancement effect



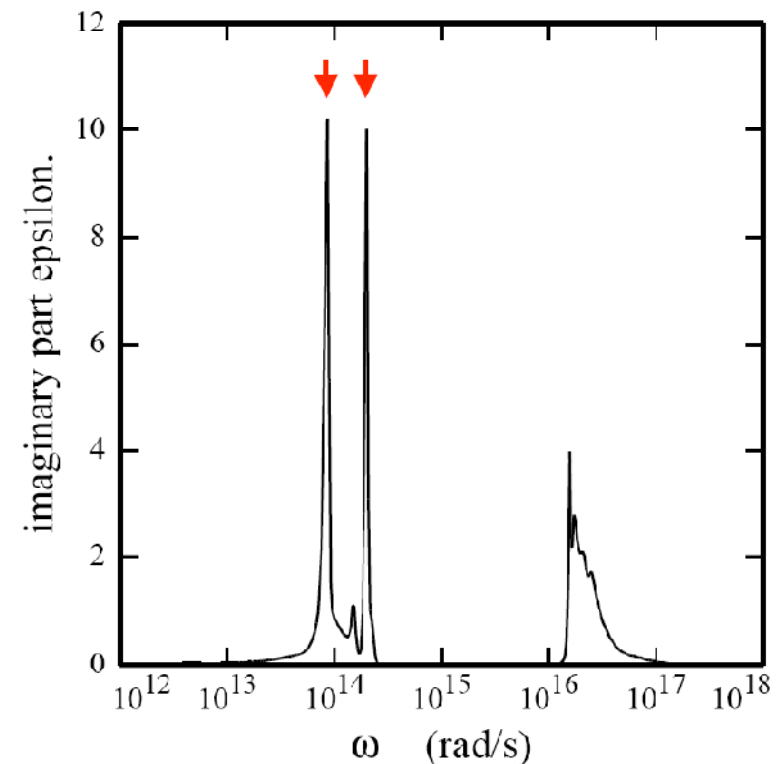
Surface waves: described by dielectric constant $\epsilon(\omega)$

Infra-red resonance

(SiC, quartz, alumine, silica, Si doped)

Radiative thermal transfer

increased by the resonance effect

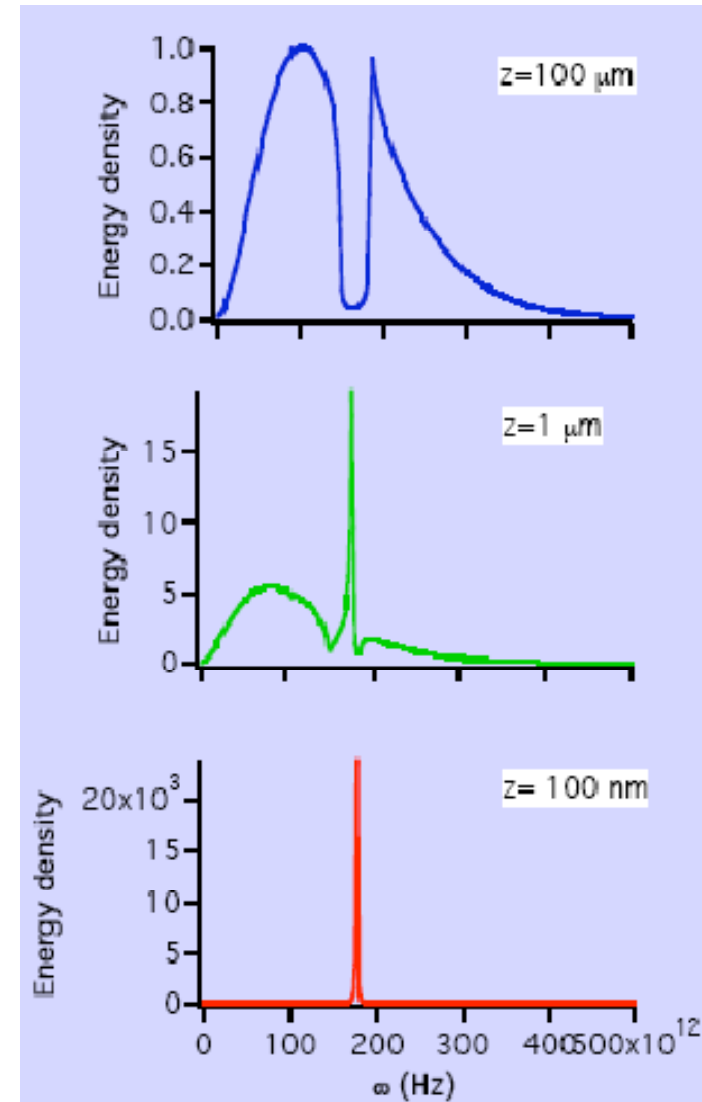


Density of energy near a SiC-vacuum interface

Far field: the energy density well reproduces the Plank black body theory

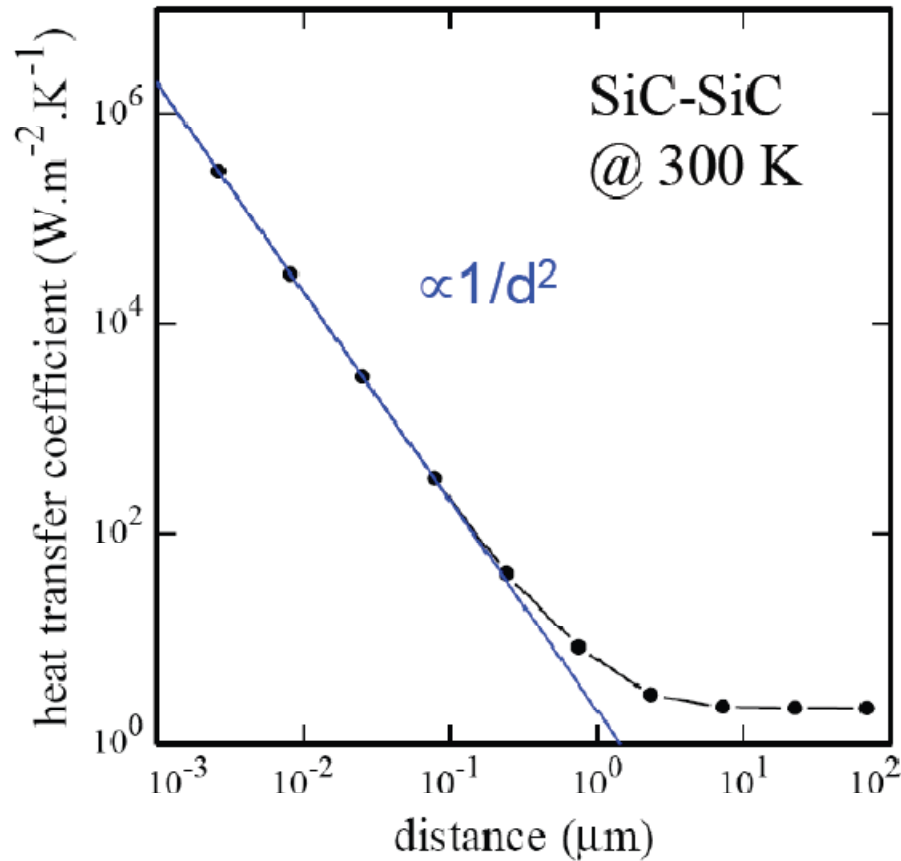
Near field: the energy density exceeds the Plank black body theory:

Monochromatic thermal emission and exponential decay with the distance

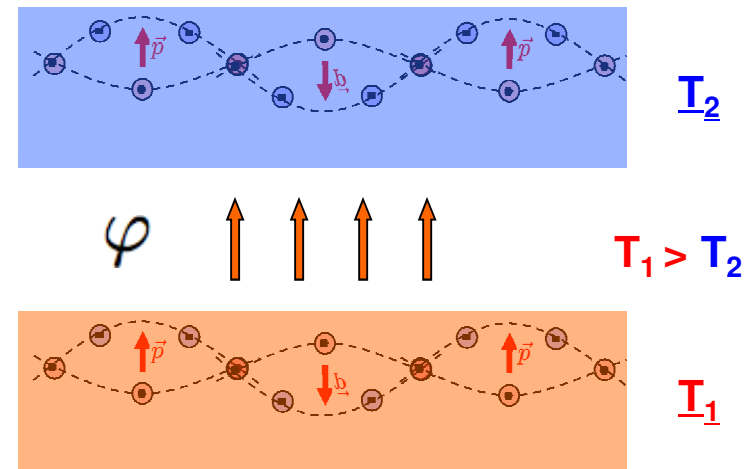


Dielectric materials: surface Phonon-Polariton enhancement effect

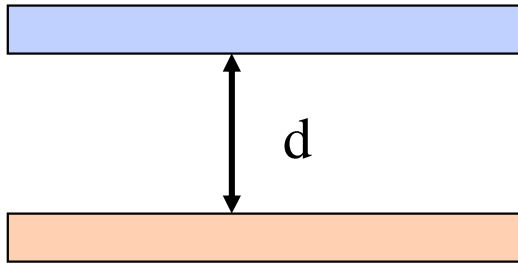
Theoretical model



Plane-Plane geometry



Plane-plane geometry: experimental issue

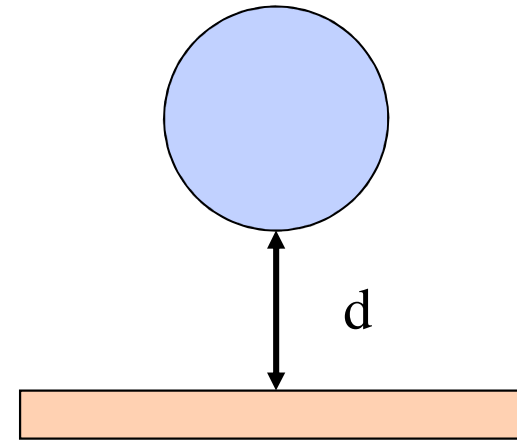


Plane-Plane

Theory developed

BUT

Experiments very difficult



Plane-sphere

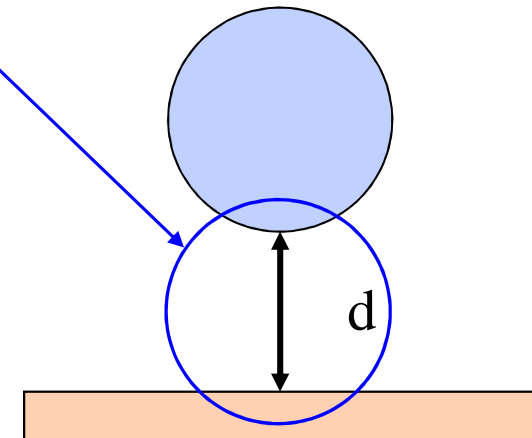
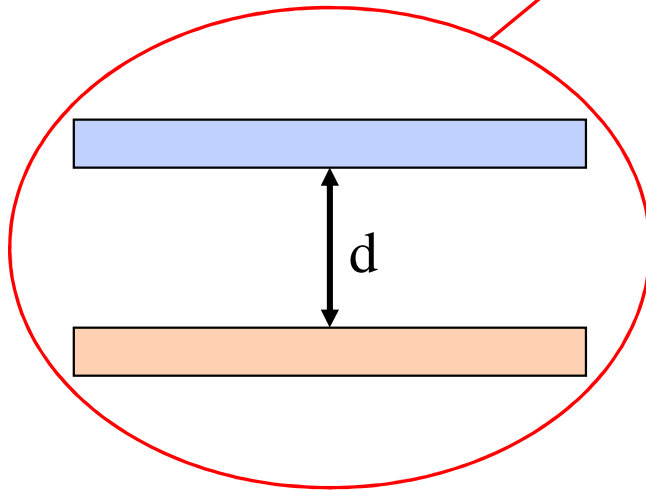
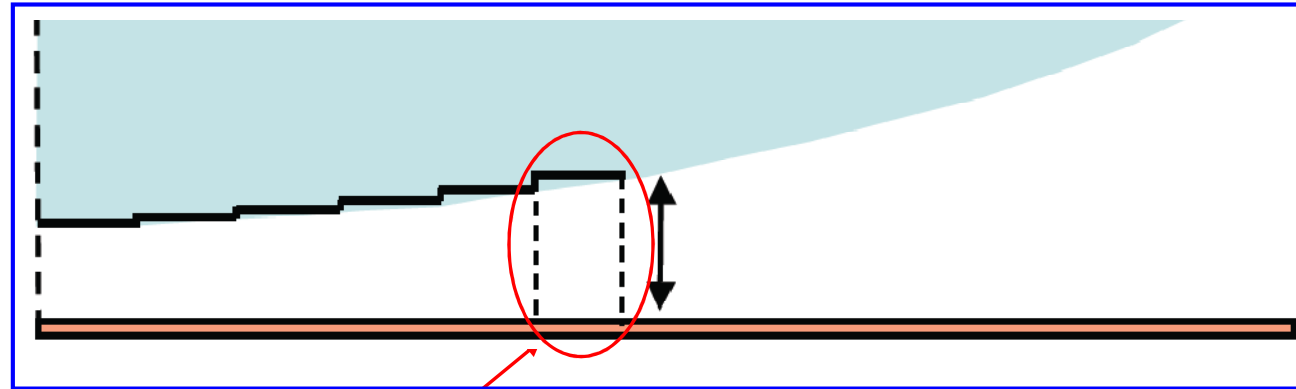
Experimentally possible

BUT

Theory not yet developed

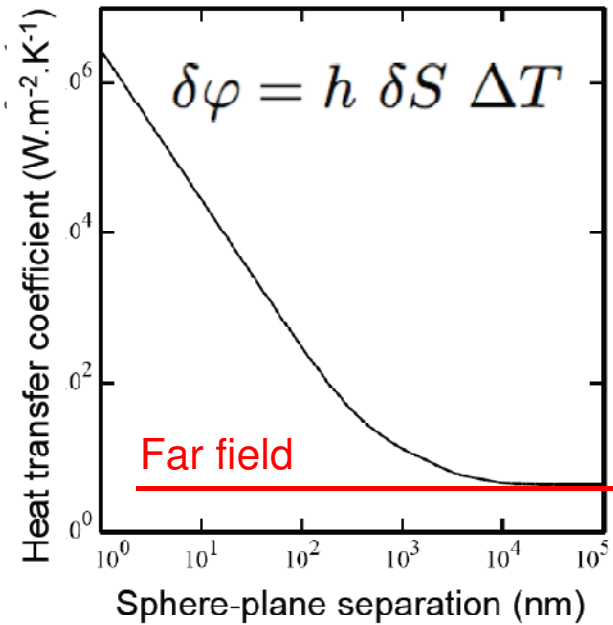
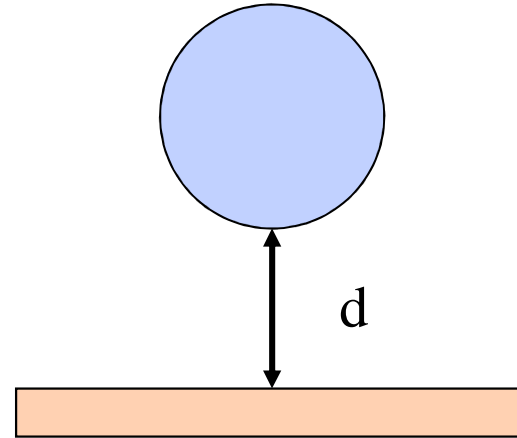
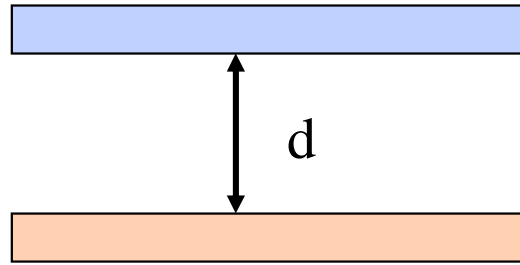
Sphere-Plane geometry: theory

Sphere-Plane geometry

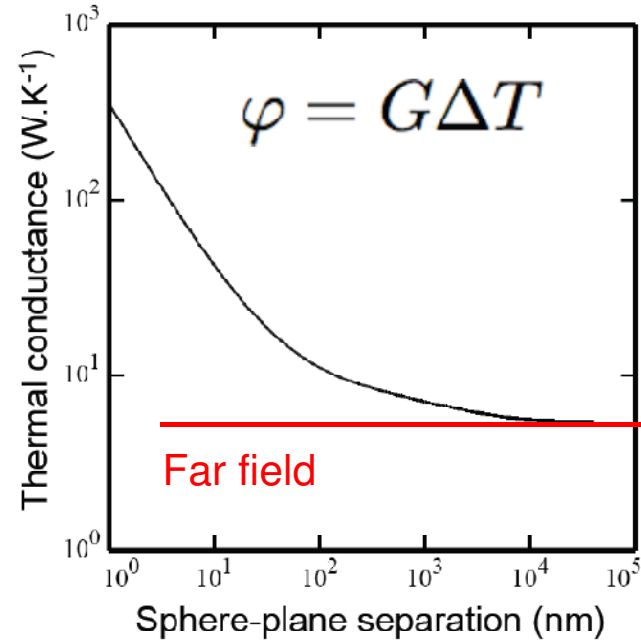


Proximity force approximation

Sphere-Plane geometry: theory

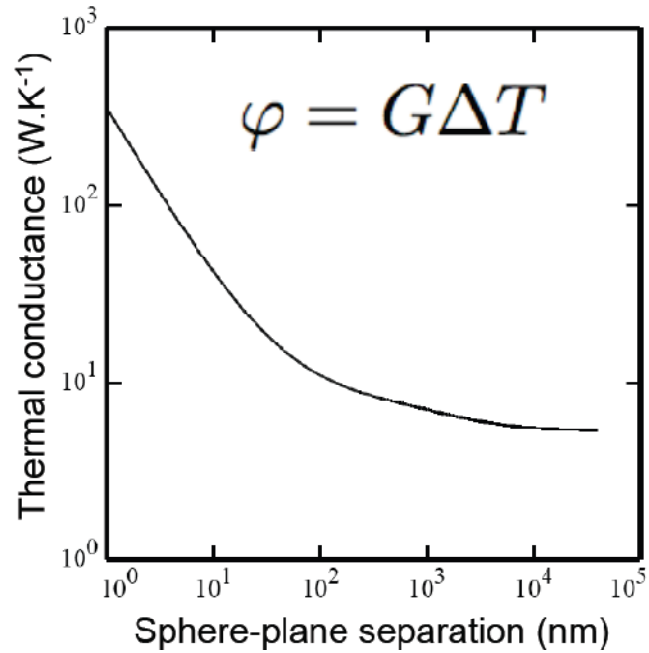


Summation



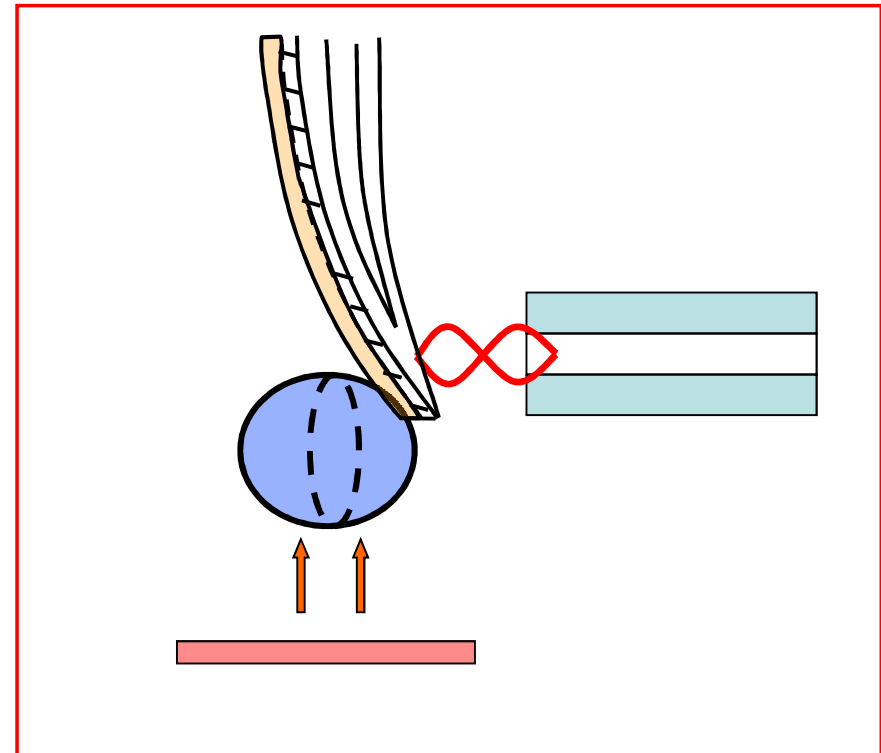
Proximity force approximation

Switch to radiative heat transfer measurement...

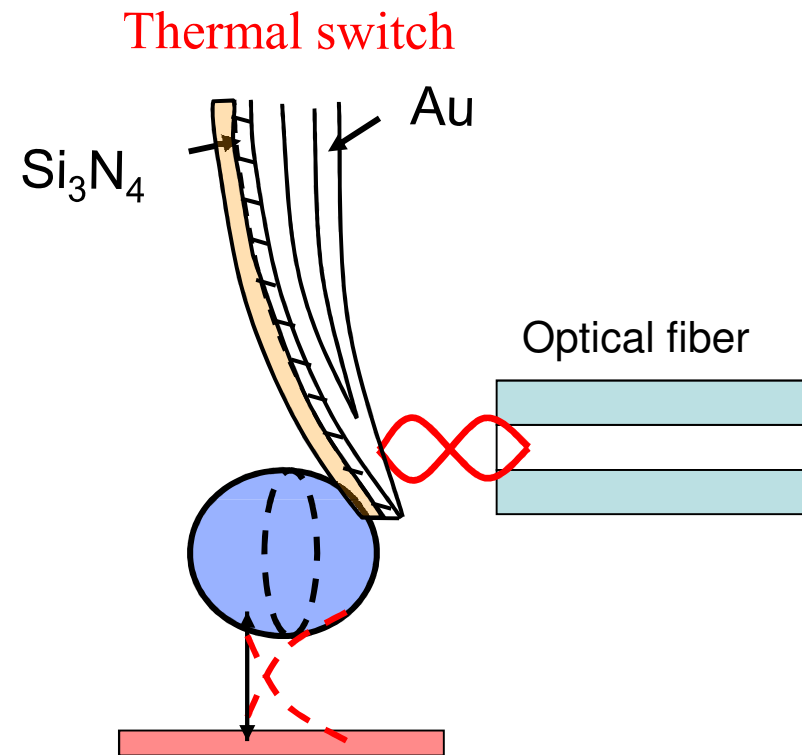
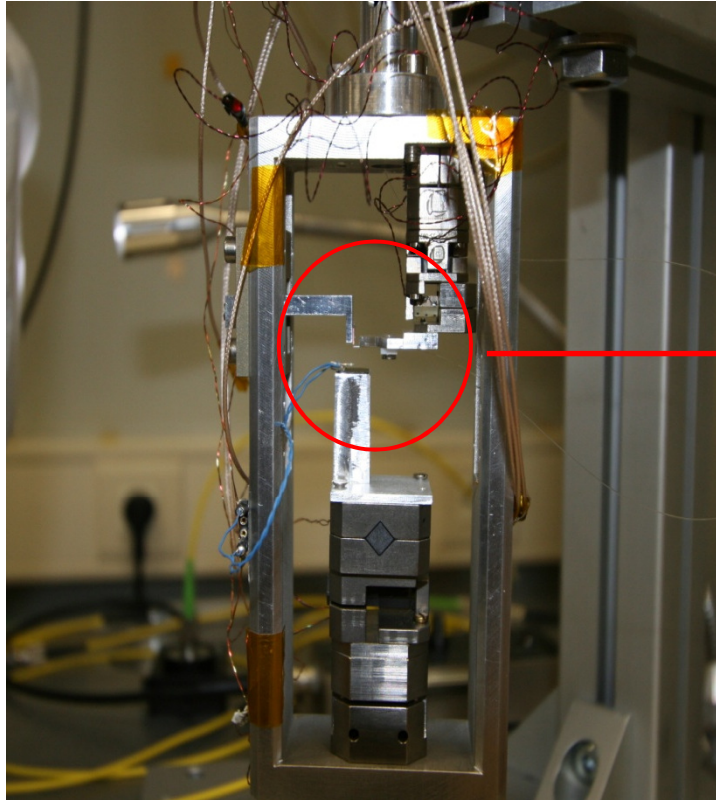


What we want to measure

How we want to measure

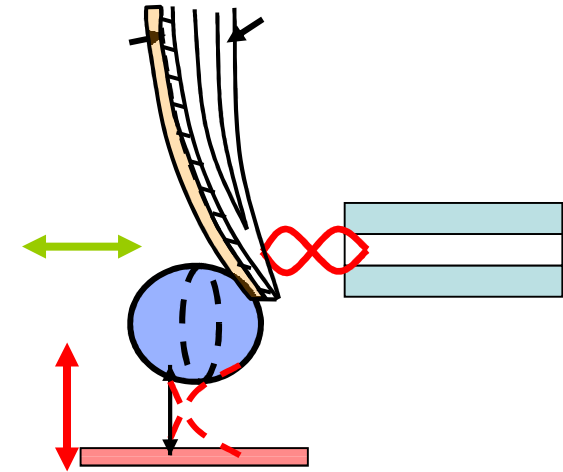
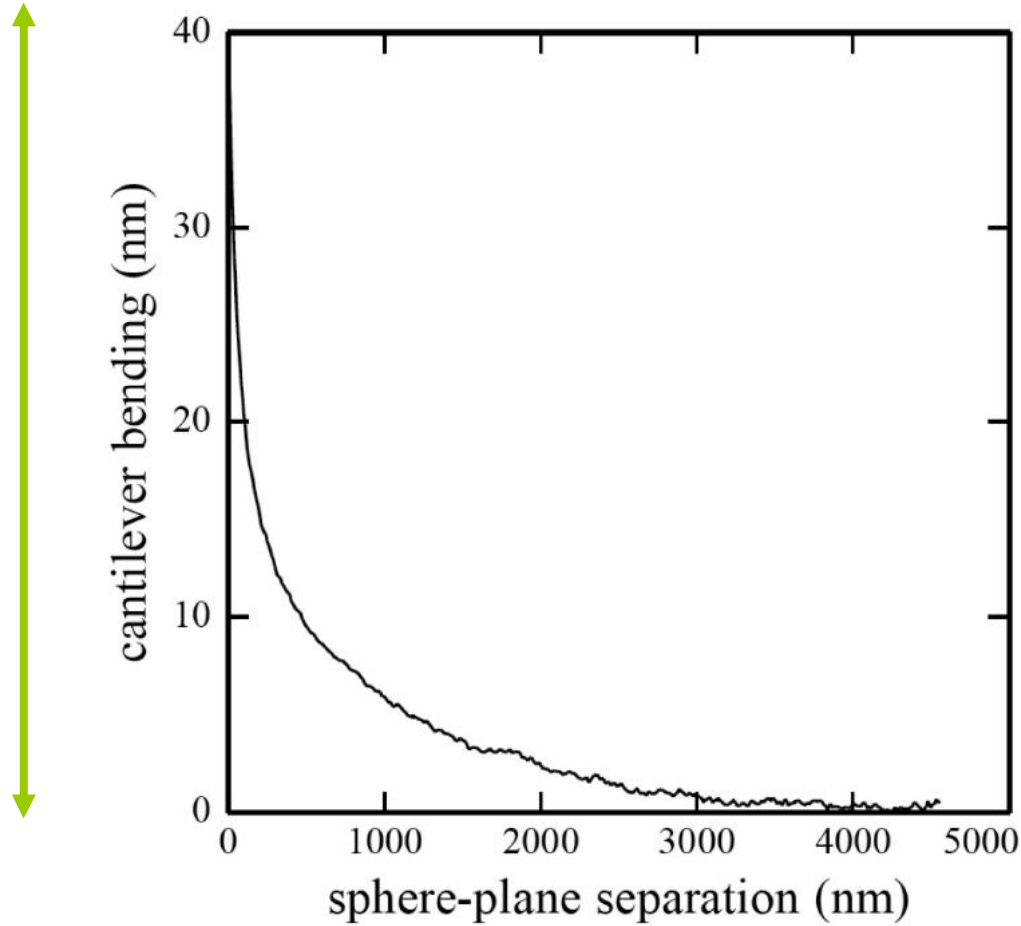


Experimental set-up



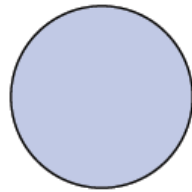
- Power exchanged = lever deflection : thermal switch effect on the lever
- High vacuum $P \sim 10^{-6}$ mbar : conduction negligible
- $\Delta T = 10\text{-}20$ K.

Calibration ???



Contact definition ???

Far-field



T_c

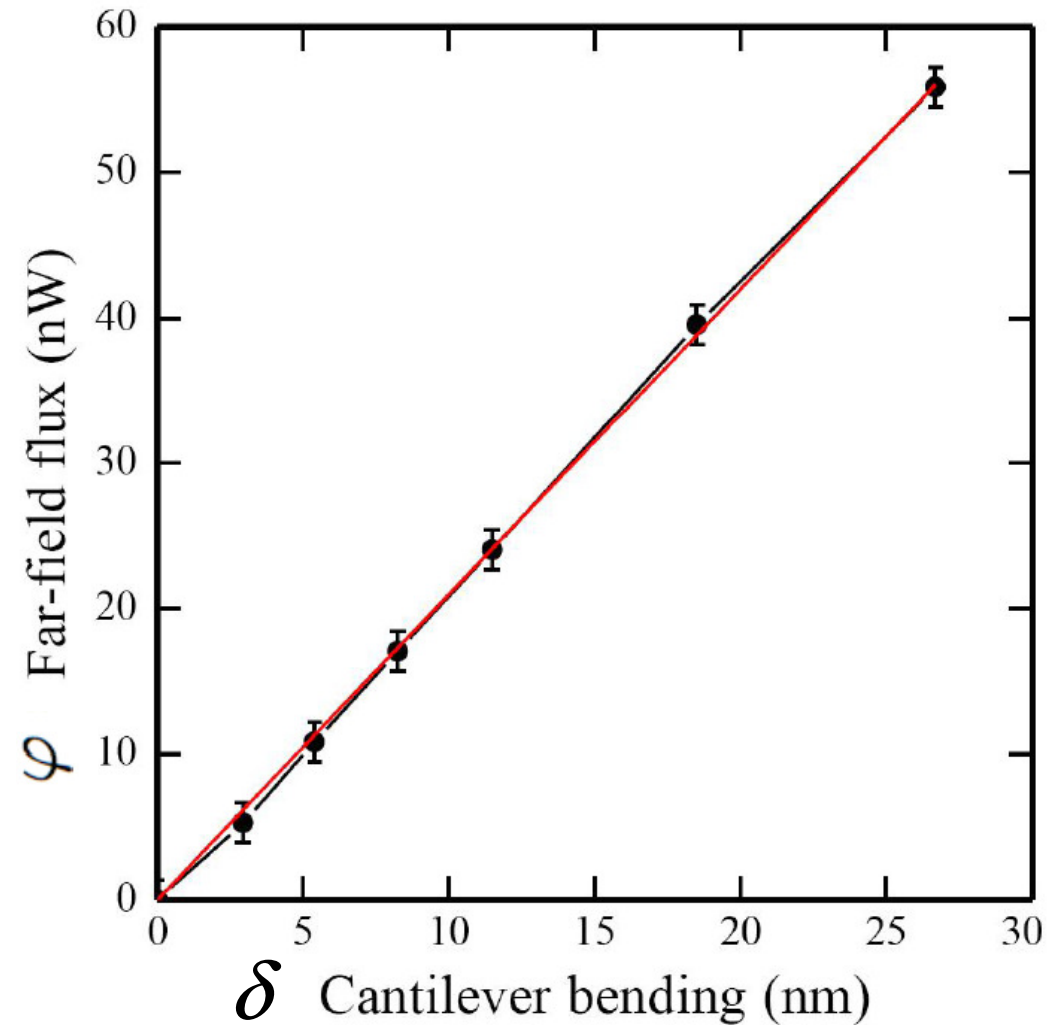


T_h

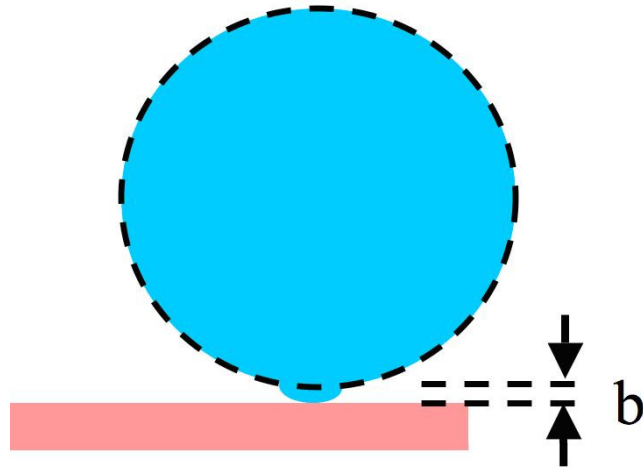
$$\varphi = 2\pi R^2 4\epsilon\sigma T^3 \Delta T$$

$$\varphi = H \cdot \delta$$

$$H = 2.03 \text{ nW / nm}$$



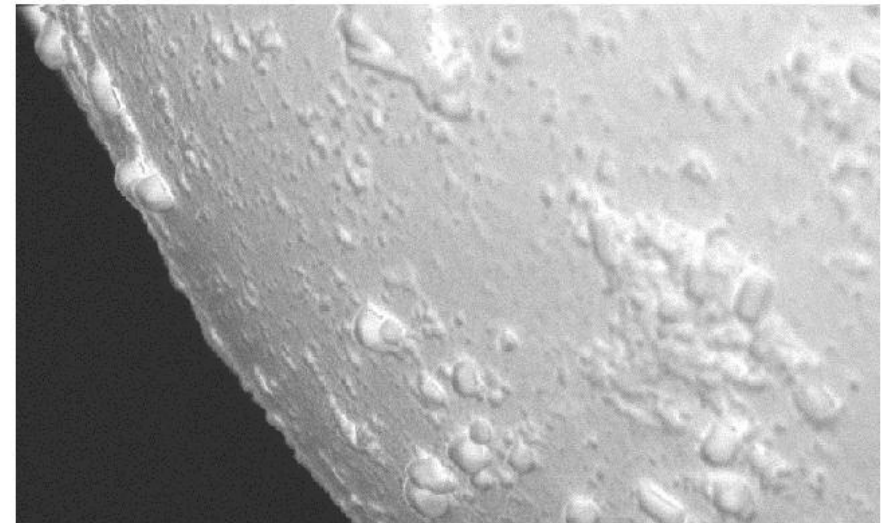
Surface roughness



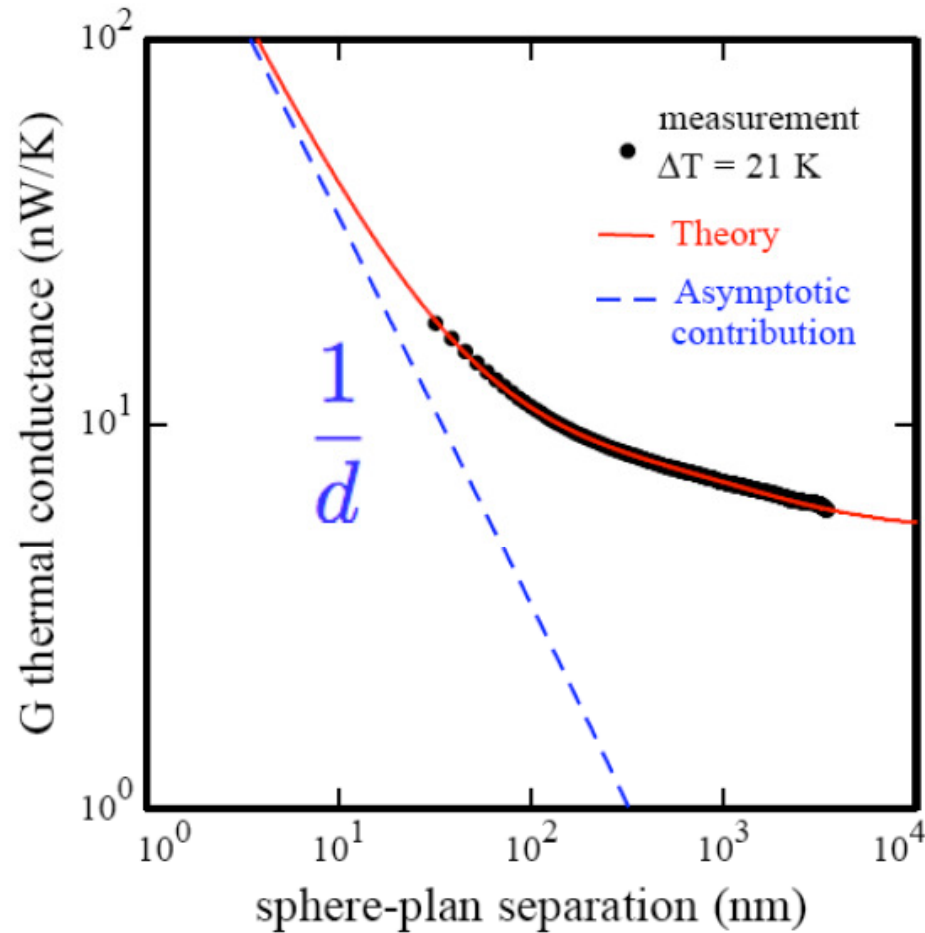
Contact between plate and
sphere asperity

Average surface contact
shifted respect hard contact

From SEM image sphere
roughness:
50 nm rms



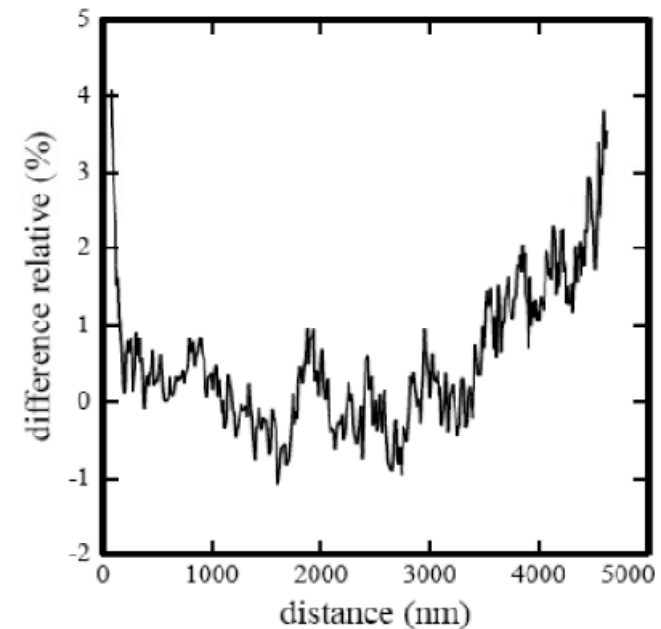
Comparison Experiments-theory



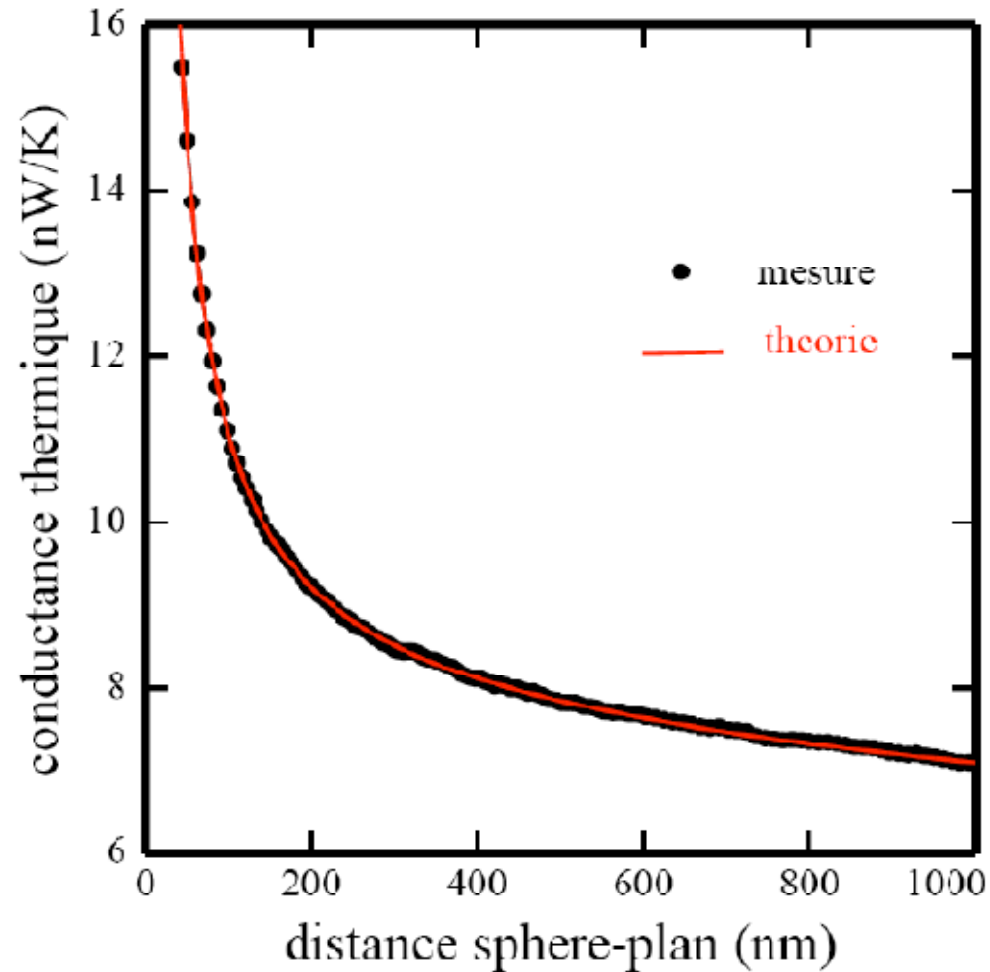
Glass sphere – glass plane

Sphere diameter 40 μm

H and b adjusted:
 $H = 2,162$ nm/nW
 $b = 31,8$ nm



Comparison Experiments-theory



Glass sphere – glass plane

Sphere diameter 40 μm

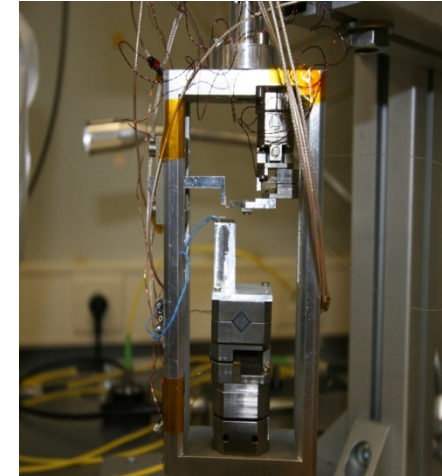
ZOOM ON NEAR-FIELD REGIME

H and b adjusted:

H = 2,162 nm/nW

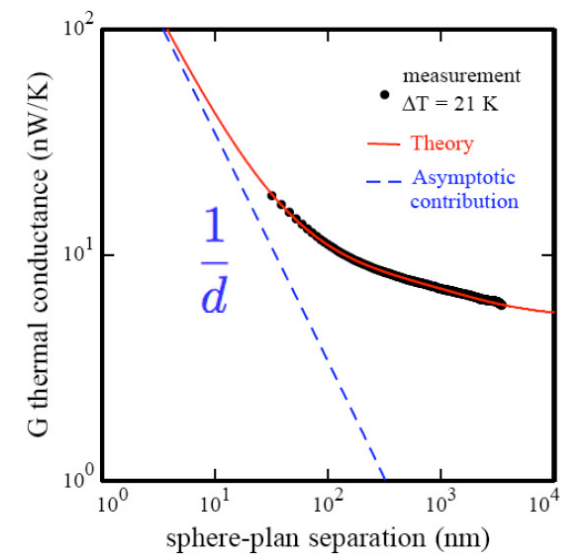
b = 31,8 nm

Development of experimental set-up for the radiative thermal transfer

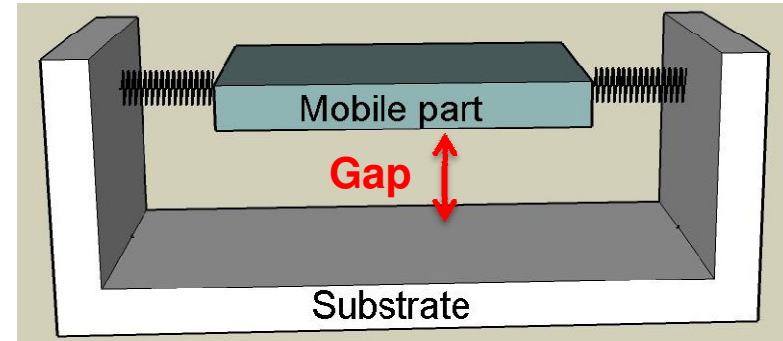


Precise measurement heat transfer in 50nm-5um range

Relative comparison theory-experience with 4% indetermination



Interaction forces in plane-plane geometry:



Dependency on distance of the major interaction forces

Hydrodynamic force (perfect slip):

$$F \rightarrow 1/d$$

Electrostatic force:

$$F \rightarrow 1/d^2$$

Thermal radiation:

$$\Phi \rightarrow 1/d^2$$

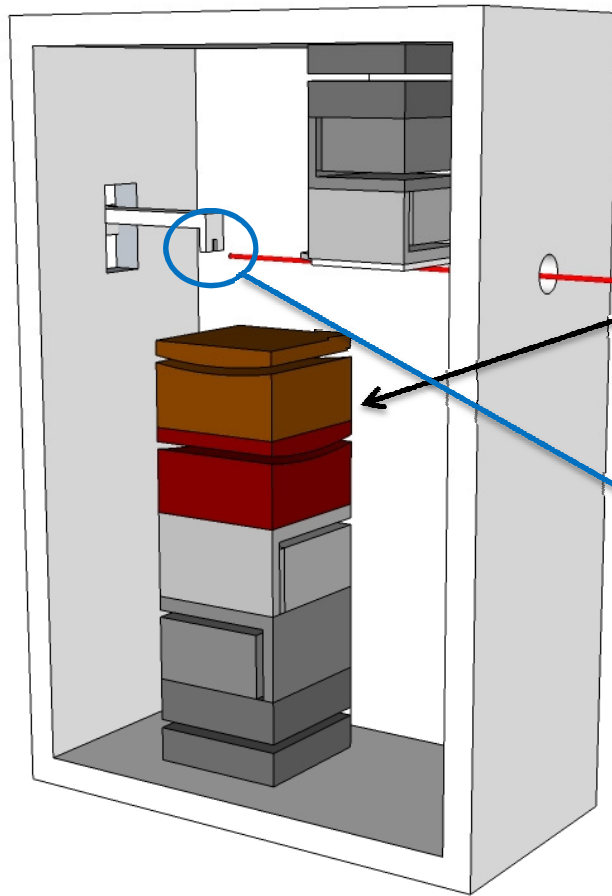
Hydrodynamic force (no slip):

$$F \rightarrow 1/d^3$$

Casimir force:

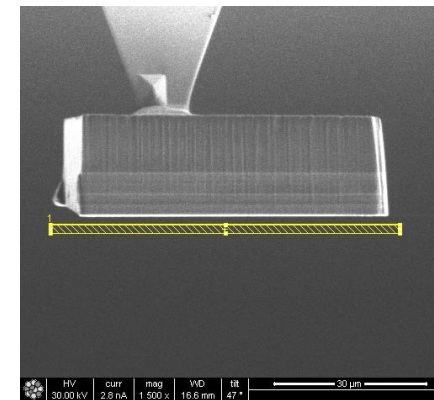
$$F \rightarrow 1/d^4$$

Set-up

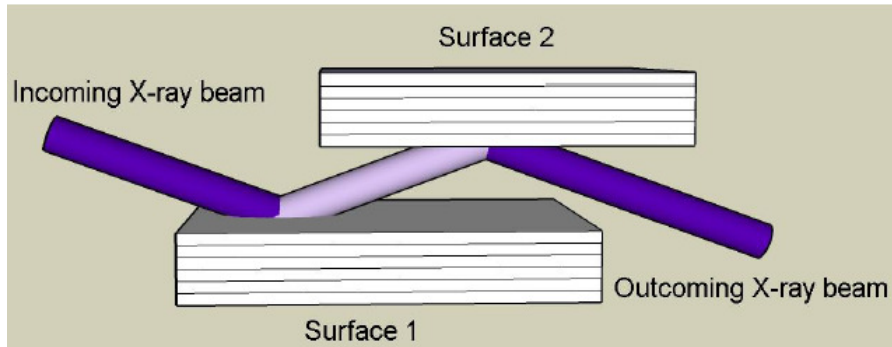


Misalignment correction
Attocube inertial motor goniometer:
 10^{-4} deg

Focused Ion Beam sample realization



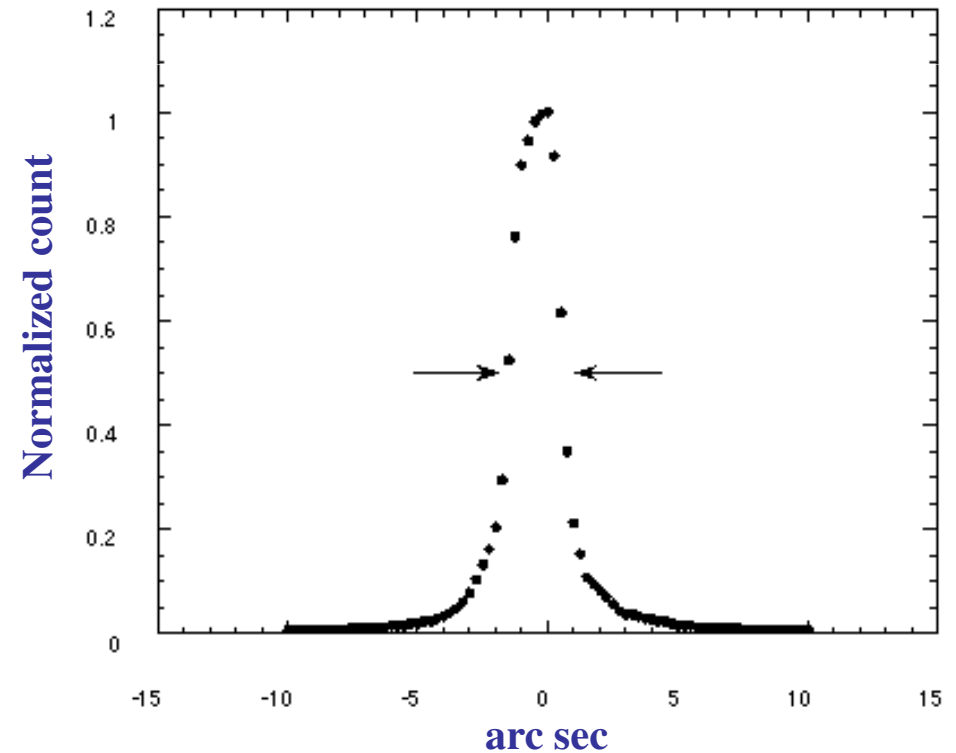
Alignment



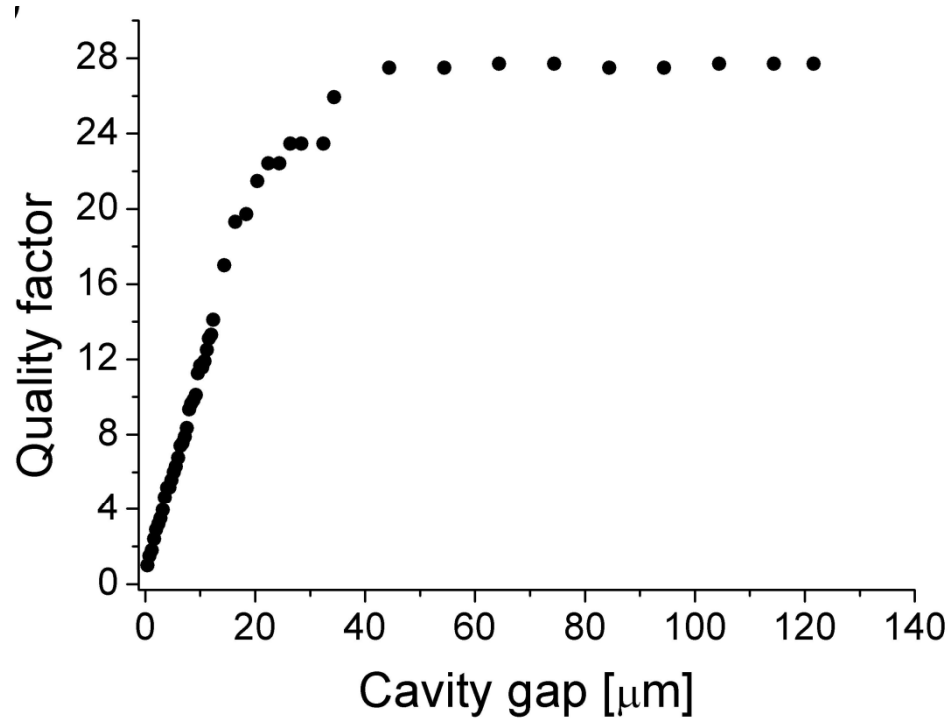
Alignment can be controlled using X-ray diffraction

The precision in angle given by the Bragg peak .

For Silicon Bragg width $\sim 10^{-4}$ deg



What happens at large gap?



Damping of the lever is not depending on distance:

WHY?

Coming back to NS equation:

$$\rho \left[\frac{\partial \vec{v}}{\partial t} \right] = \eta \nabla^2 \vec{v} - \nabla p$$

Boundary layer definition: $d_L = \sqrt{\frac{2\eta}{\rho\omega}}$

$$d \gg d_L \Rightarrow \rho \left[\frac{\partial \vec{v}}{\partial t} \right] \gg \eta \nabla^2 \vec{v}$$

Damping should saturate

Fluctuation-dissipation theorem:

$$\left\langle j_m^f(\vec{r}, \omega) j_n^f(\vec{r}', \omega')^* \right\rangle = 2 \frac{\omega \epsilon_0}{\pi} \epsilon''(\omega) \Theta(\omega, T) \delta_{m,n} \delta(\vec{r} - \vec{r}') \delta(\omega - \omega')$$

Green Tensor formalism:

$$\vec{E}(\vec{r}, \omega) = (i\omega\mu_0) \vec{G}^E(\vec{r}, \vec{r}', \omega) \cdot \vec{j}^f(\vec{r}', \omega)$$

$$\vec{H}(\vec{r}, \omega) = \vec{G}^H(\vec{r}, \vec{r}', \omega) \cdot \vec{j}^f(\vec{r}', \omega)$$

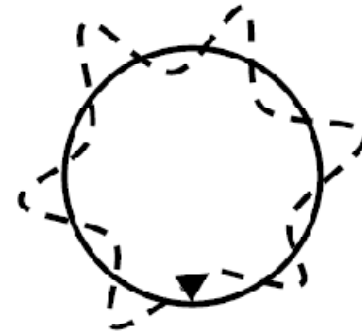
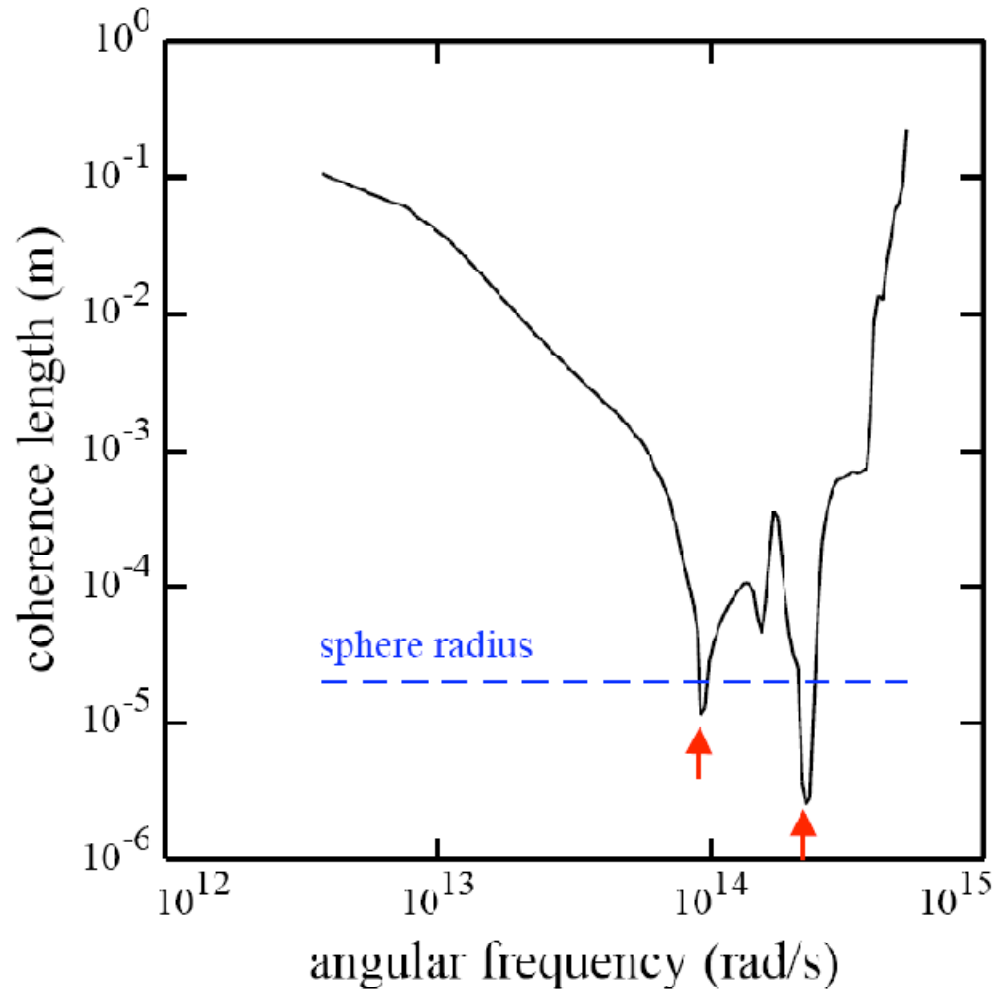
Electromagnetic energy density:

$$u(\vec{r}, \omega, t) = \frac{\epsilon_0}{2} \left\langle \vec{E}(\vec{r}, \omega) \cdot \vec{E}(\vec{r}, \omega)^* \right\rangle + \frac{\mu_0}{2} \left\langle \vec{H}(\vec{r}, \omega) \cdot \vec{H}(\vec{r}, \omega)^* \right\rangle$$

$$u(z, \omega, t) = \frac{1}{4} \frac{\omega^2 \Theta(\omega, T)}{\pi^2 c^2} \int_0^{k_0} \frac{K dK}{k_0 |\gamma_0|} \frac{1}{2} \left[\left(1 - |r_s|^2\right) + \left(1 - |r_p|^2\right) \right] +$$

$$+ \frac{\omega^2 \Theta(\omega, T)}{\pi^2 c^2} \int_{k_0}^{\infty} \frac{K^3 dK}{k_0^3 |\gamma_0|} \frac{1}{2} \left[\text{Im}(r_s) + \text{Im}(r_p) \right] e^{-2\gamma_0'' z}$$

More about Derjaguin approximation

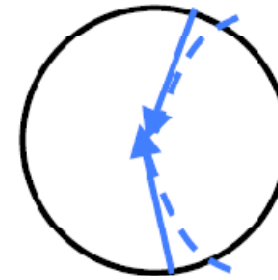
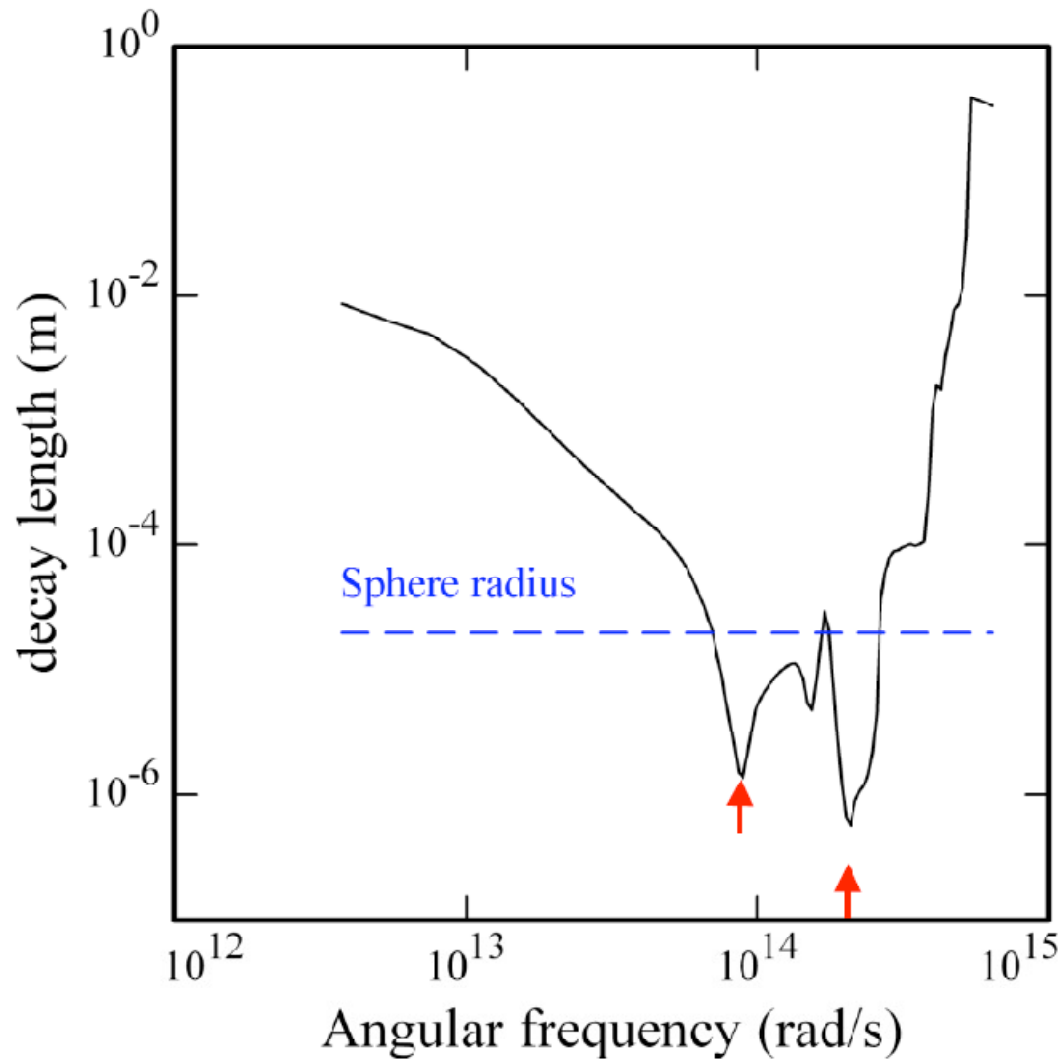


No Mie scattering

No interferences

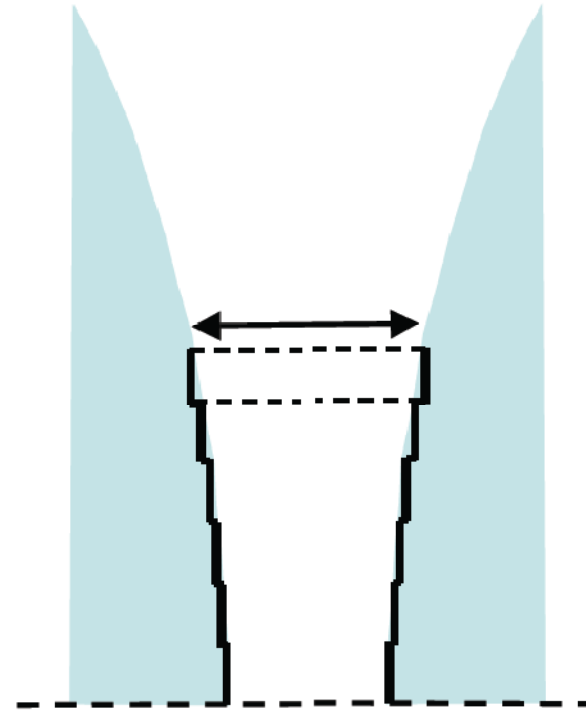
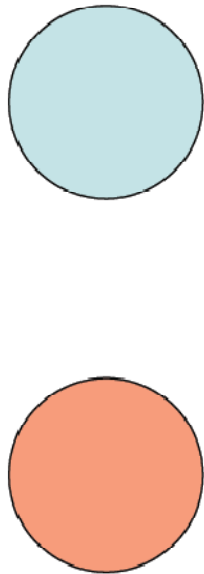
2 points of the sphere:
may be considered as
independent

More about Derjaguin approximation



More about Derjaguin approximation

Radiative heat transfer between two spheres.

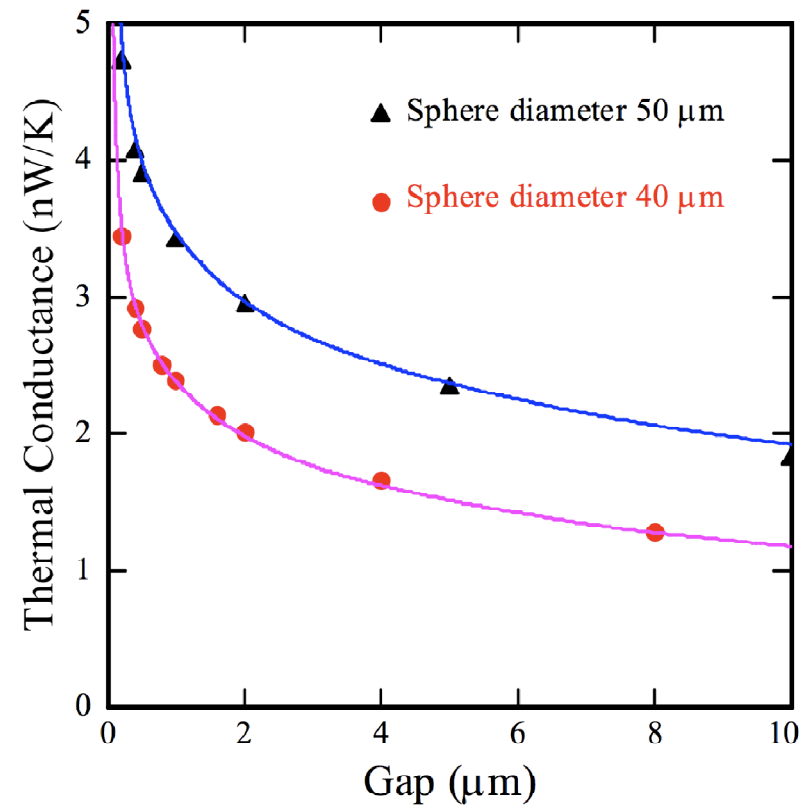
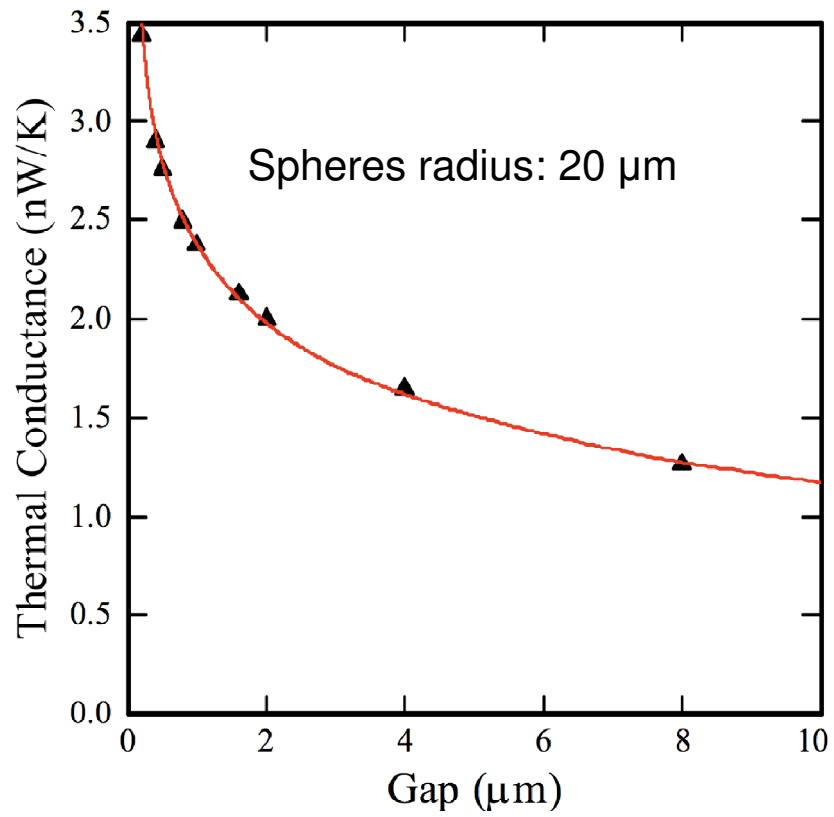


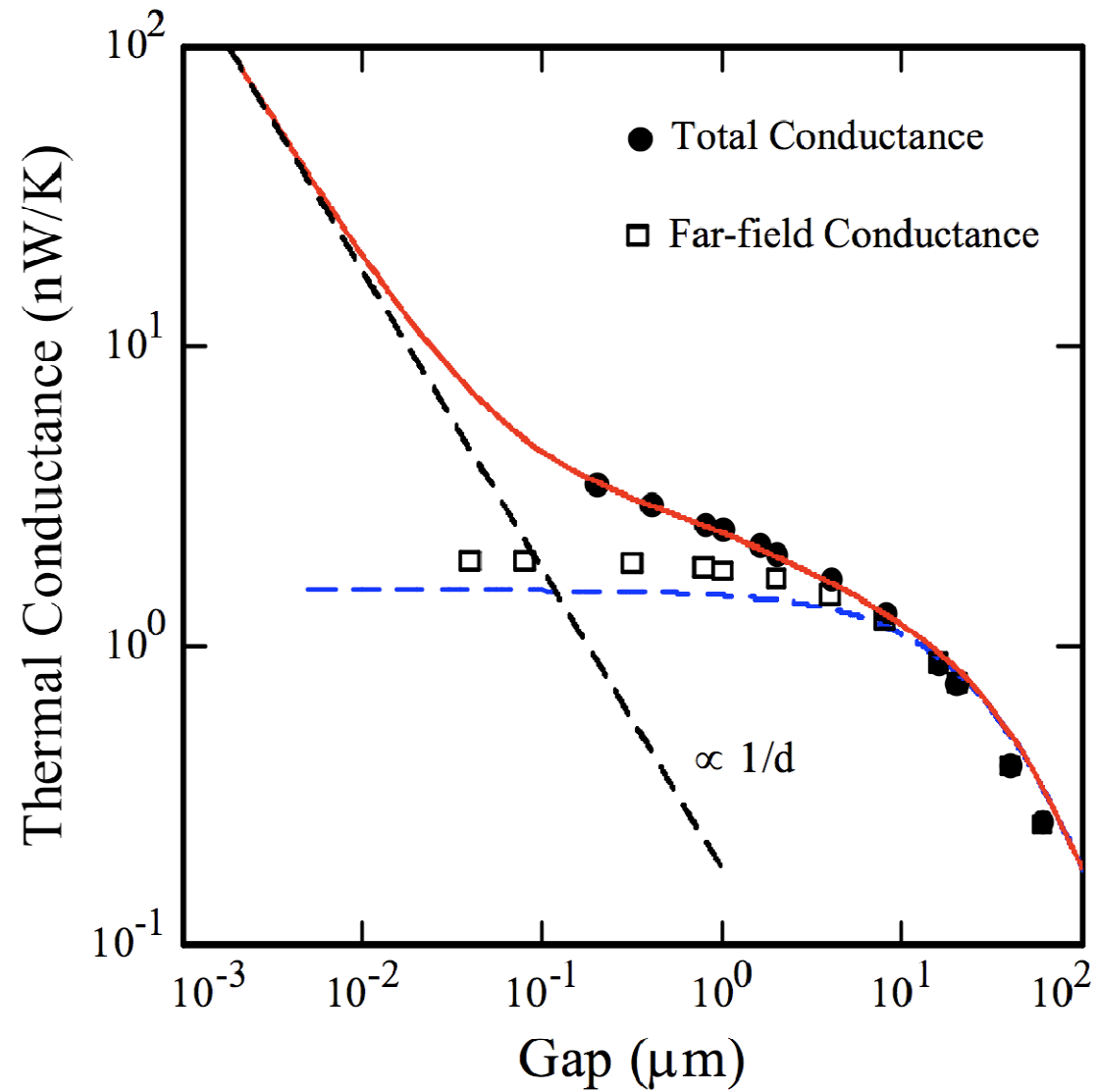
Can be computed exactly

PRB 77, 075125

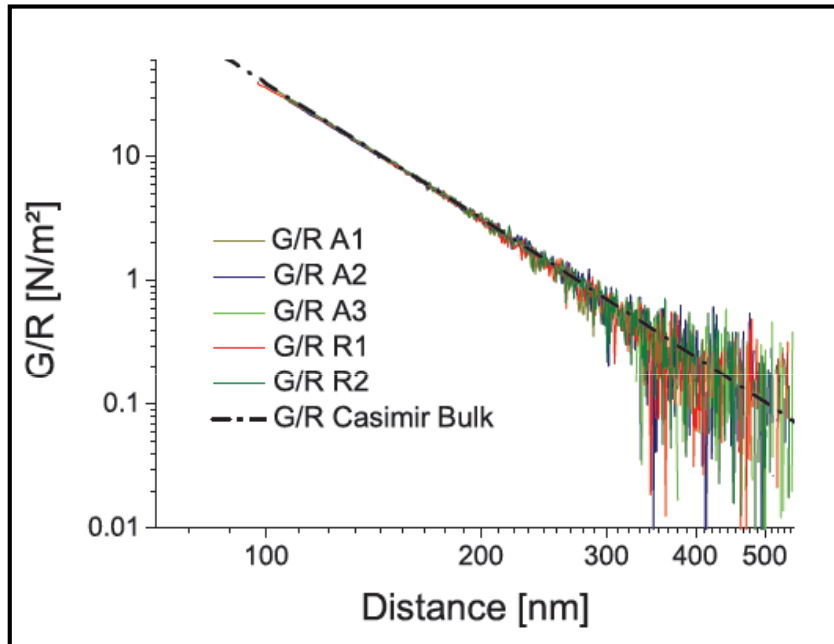
Far-field: view factor

Near-field: Derjaguin approximation

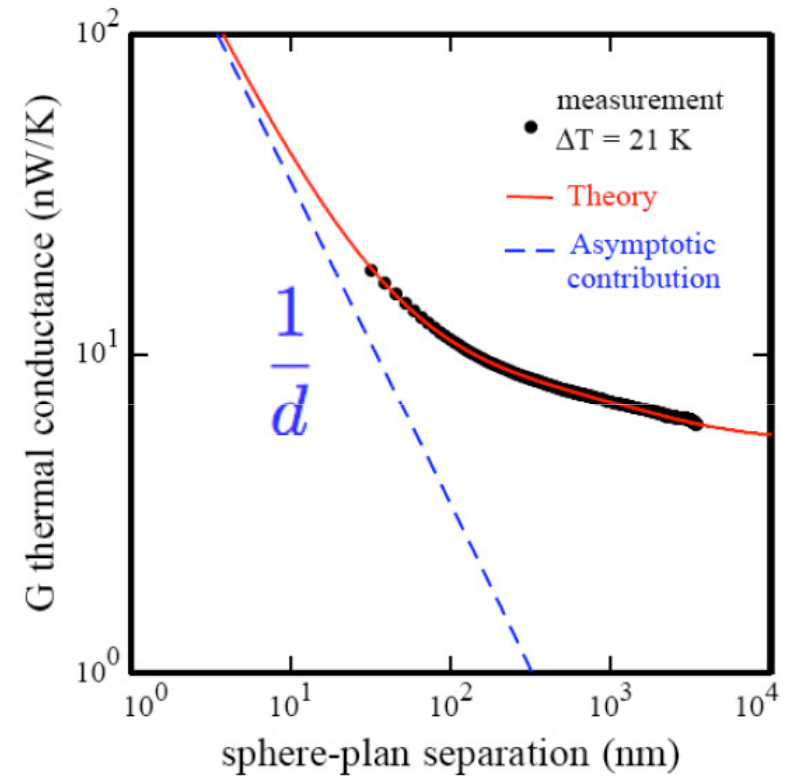




Casimir force and radiative heat transfer: same origin, same experimental set-up



Jourdan *et al*, 2007



Siria *et al*, 2009